Revision of the *Eurycea quadridigitata* (Holbrook 1842) Complex of Dwarf Salamanders (Caudata: Plethodontidae: Hemidactyliinae) with a Description of Two New Species

Author(s): Kenneth P. Wray, D. Bruce Means, and Scott J. Steppan
Source: Herpetological Monographs, 31(1):18-46.
Published By: The Herpetologists' League
DOI: http://dx.doi.org/10.1655/HERPMONOGRAPHS-D-16-00011
URL: http://www.bioone.org/doi/full/10.1655/HERPMONOGRAPHS-D-16-00011

Herpetological Monographs, 31, 2017, 18–46

Revision of the *Eurycea quadridigitata* (Holbrook 1842) Complex of Dwarf Salamanders (Caudata: Plethodontidae: Hemidactyliinae) with a Description of Two New Species

Kenneth P. Wray[1,3], D. Bruce Means[1,2], and Scott J. Steppan[1]

[1] Department of Biological Science, Florida State University, Tallahassee, FL 32306-4295, USA
[2] Coastal Plains Institute and Land Conservancy, 1313 Milton Street, Tallahassee, FL 32303-5512, USA

Abstract: The *Eurycea quadridigitata* complex is currently composed of the nominate species and *E. chamberlaini*, with no other species recognized. However, recent molecular studies have revealed at least five genetic lineages within this species complex, with one lineage more closely related to the neotenic *Eurycea* species of central Texas and *E. chamberlaini* nested within *E. quadridigitata* sensu lato. We use large-scale geographic sampling in combination with a multilocus species delineation method and morphology to test whether these genetic lineages represent distinct species under the general lineage concept of species. We describe two new species of salamander from this complex, resurrect and elevate a former subspecies to full species status, add to the diagnosis of *E. chamberlaini*, and redefine *E. quadridigitata* in the context of this revision. All five species are diagnosable from one another through a number of meristic, morphometric, molecular, and ecological criteria.

Key words: Amphibian; Caudata; *Eurycea*; *Eurycea chamberlaini*; *Eurycea hillisi* sp. nov.; *Eurycea paludicola*; *Eurycea sphagnicola* sp. nov.; Salamander; Southeastern Coastal Plain; Systematics

The dwarf Salamanders (*Eurycea quadridigitata*; Holbrook 1842) are a small species of plethodontid that occur throughout the Southeastern United States, ranging from the eastern third of Texas through southern Arkansas, Louisiana, the southern portions of Mississippi, Alabama, and Georgia, most of Florida, and the coastal lowlands of the Carolinas (Petranka 1998). Long considered a color morph of *E. quadridigitata*, the recently described Chamberlain's Dwarf Salamanders (*E. chamberlaini*) are known only from the Piedmont of North and South Carolina and near the central coast of North Carolina (Harrison and Guttman 2003). Together, these two salamander species are differentiated from all other members of the genus by having four digits on the hind feet (five in all other *Eurycea*). These salamanders are also much more terrestrial than other members of the genus, often found far from permanent water. In fact, *E. quadridigitata* is commonly the only plethodontid salamander where it occurs (Means 2000). Like other members of the genus, these two species have a biphasic lifecycle but, unlike other *Eurycea* which breed in lotic (= flowing) aquatic habitats, *E. chamberlaini* is also known to occasionally breed in lentic (= non–flowing or sluggish) aquatic habitats while *E. quadridigitata* breeds exclusively in lentic habitats. In these habitats, eggs are laid in water where they hatch and the larvae remain through metamorphosis (Petranka 1998). Perhaps due to breeding in such highly variable and ephemeral systems, *E. chamberlaini* and *E. quadridigitata* have greatly reduced larval periods when compared to other *Eurycea* species, sometimes transforming in as little as 2 mo (as long as 2 yr in some other *Eurycea*; Petranka 1998; Means 2000).

Most of the taxonomic changes in this species complex have involved the generic placement of *E. quadridigitata*. First described by Holbrook (1842) as *Salamandra quadridigitata*, this species was soon placed in the genus *Batrachoseps* (Baird 1849) and then *Manculus* (Cope 1869). Dunn (1923) was the first to place the species in the genus *Eurycea*, though Mittleman (1947, 1967) continued to recognize *Manculus*. Using a number of osteological characters, Wake (1966) placed *Manculus* back in the synonymy of *Eurycea*, which was later confirmed by molecular data (Chippindale et al. 2000), where it has remained since.

Despite the large geographic range of *E. quadridigitata*, prior to the description of *E. chamberlaini* very little variation had been described, none of which is currently recognized taxonomically. Cope (1871) first described *Manculus remifer* from a single specimen collected from the vicinity of Jacksonville, Florida. However, this taxon was later relegated to subspecific status by Stejneger and Barbour (1923; as *M. q. remifer*) and Dunn (1923; as *E. q. remifer*). In the first major review of the species, Mittleman (1947), recognizing the genus *Manculus*, was unable to find any character separating *M. q. remifer* from *M. q. quadridigitatus* and, therefore, synonymized the former. Based on the geographic distribution of vomerine teeth, costal groove counts, and the number of costal grooves between adpressed limbs, Mittleman (1947) redefined the subspecies *M. q. quadridigitatus* while describing the new subspecies *M. q. paludicolus* from Grant Parish, Louisiana and *M. q. uvidus* from Caddo Parish, Louisiana. Despite his earlier review, Mittleman (1967) no longer recognized any subspecies, referring to earlier variation as not being correlated with geography or simply clinal in nature. Currently, *E. quadridigitata* and *E. chamberlaini* are recognized as monotypic.

Recent molecular studies have shown that several genetic lineages exist within *E. quadridigitata* sensu lato (Kozak et al. 2009; Lamb and Beamer 2012; Bonett et al. 2014; Wray and Steppan 2016). Kozak et al. (2009) first suggested that *E. quadridigitata* sensu lato was paraphyletic with respect to the neotenic *Eurycea* on the Edwards Plateau of Texas, with an individual of *E. quadridigitata* from South Carolina sister to the *E. bislineata* complex while an individual from Mississippi was sister to the Texas neotenes. In the first comprehensive study of the group, Lamb and Beamer (2012)

[3] Correspondence: e-mail, kwray@bio.fsu.edu

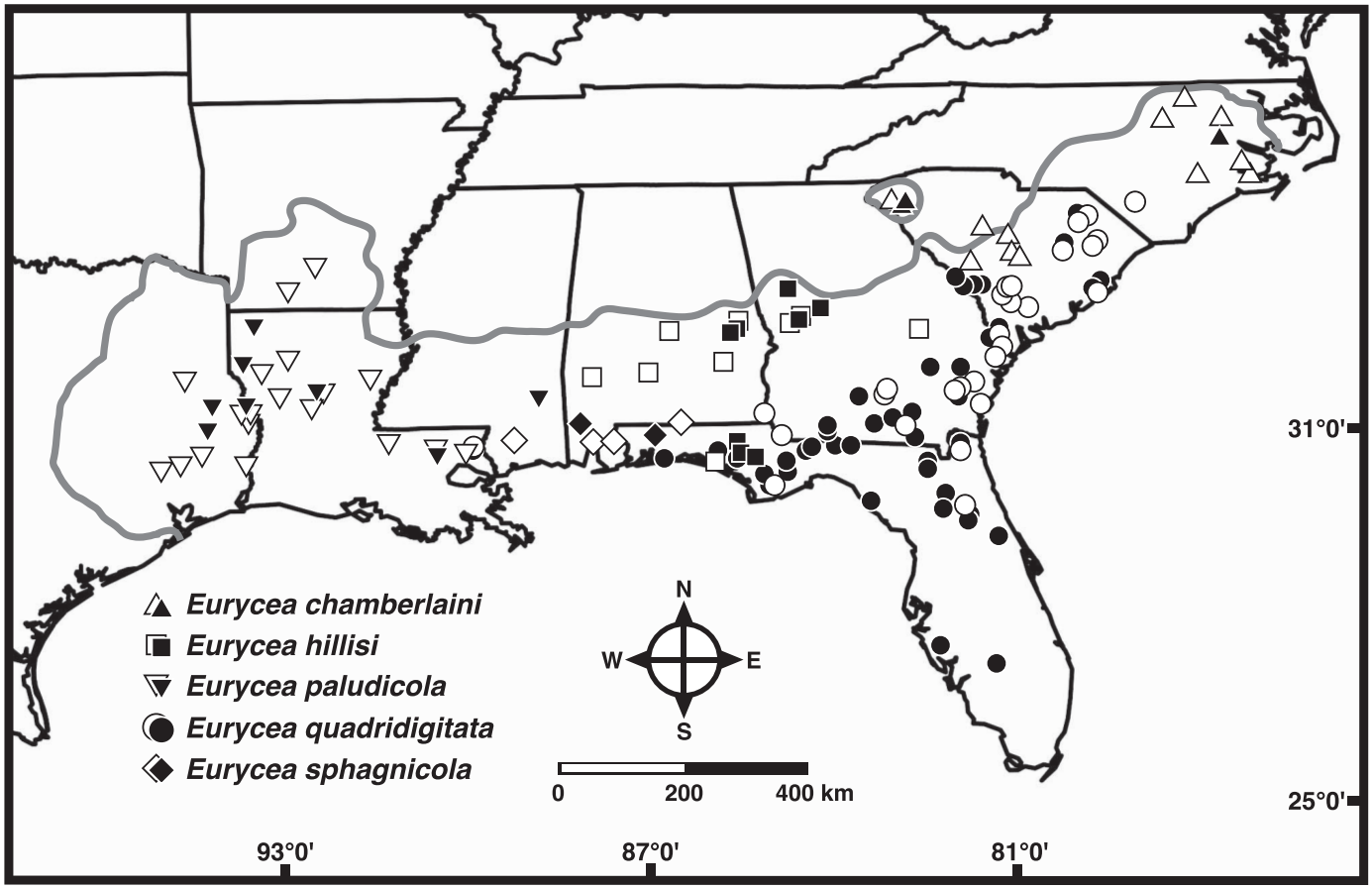

FIG. 1.—Geographic distribution of the *Eurycea quadridigitata* complex determined by genetic analyses from two previous studies. Solid symbols represent samples from this study. Open symbols represent samples from Lamb and Beamer (2012; *E. paludicola* = western lineage of Lamb and Beamer, *E. hillisi* = central lineage of Lamb and Beamer, *E. sphagnicola* = Florida Panhandle lineage of Lamb and Beamer). Gray line indicates the historic range of *E. quadridigitata* sensu lato.

used 120 samples of the *E. quadridigitata* complex and portions of three mitochondrial (16S ribosomal RNA, cytochrome B, and NADH dehydrogenase subunit 2) and two nuclear (proopiomelanocortin and recombination activating 1) genes to show that (1) five distinct clades existed within the complex; (2) *E. chamberlaini* rendered *E. quadridigitata* sensu lato paraphyletic; and (3) confirmed that western *E. quadridigitata* were more-closely related to the Texas neotenes. Using different data sets and methods, Bonett et al. (2014) and Wray and Steppan (2016) confirmed these results.

Using representative samples from all of the clades in Lamb and Beamer (2012) and a nearly complete phylogeny of the Spelerpini, Wray and Steppan (2016) estimated the divergence times among the *E. quadridigitata* complex. They found the divergence between the western *E. quadridigitata* and the eastern *E. quadridigitata* + *E. chamberlaini* to be between 34–19 million years ago (Ma). The divergence time between *E. chamberlaini* and its sister *E. quadridigitata* clade was estimated at 27–15 Ma, with various other eastern *E. quadridigitata* clades diverging even earlier than this.

As had been suggested by previous work, Wray and Steppan (2016) found the western populations of *E. quadridigitata* (herein referred to as the "western clade") to be more-closely related to the neotenic *Eurycea* species from the Edwards Plateau, having diverged from other *E. quadridigitata* at least 19 Ma. The remaining four lineages of *E. quadridigitata* occur east of the Mississippi River and are represented by *E. quadridigitata*, *E. chamberlaini*, a clade that breeds in hillside seepages (herein referred to as the "hillside seepage clade"), and a clade that breeds in steepheads and ravines (herein referred to as the "steephead/ravine clade"). Members of all four clades overlap in some areas (Fig. 1), but each appears to utilize distinctive breeding habitats with no evidence of interbreeding.

Herein, we use a multilocus gene tree–species tree phylogenetic approach in combination with a Bayesian coalescent species delimitation method to show that these deep genetic divergences in the *E. quadridigitata* complex represent multiple species (Rannala and Yang 2003; Yang and Rannala 2010). We then use a combination of morphological and molecular characters measured from the specimens used in the species delimitation analysis and from additional museum specimens collected at the same geographic sites to define two new species in the *E. quadridigitata* complex, resurrect and elevate a formerly recognized subspecies to species status, and redefine *E. quadridigitata* and *E. chamberlaini*.

TABLE 1.—Primers and PCR protocols used in amplification and sequencing.

Primer	Gene	Primer sequence (5′→3′)	Anneal temperature (time)	Elongation time	Cycles	Reference
MVZ15	CytB	GAACTAATGGCCCACACWWTACGNAA	50°C (30 s)	90 s	×30	Moritz et al. 1992
MVZ16R	CytB	AAATAGGAARTATCAYTCTGGTTTRAT	50°C (30 s)	90 s	×30	Moritz et al. 1992
PGludg2	CytB	GGTCTGAAAAACCAATGTTGTATTC	50°C (30 s)	90 s	×30	Wiens et al. 2006
L4437	ND2	AAGCTTTCGGGCCCATACC	50°C (35 s)	150 s	×25	Macey et al. 1997
H6159	ND2	GCTATGTCTGGGGCTCCAATTA	50°C (35 s)	150 s	×25	Weisrock et al. 2001
EqND2FI*	ND2	GGAGGCCTAAATCAACCACA	50°C (35 s)	150 s	×25	This study
EqND2RI*	ND2	GTGATGTGGTGTACGCAAGG	50°C (35 s)	150 s	×25	This study
EuryceaRag1F	RAG1	GGTAYGATGTTGCATTGGTTGCCA	58°C (30 s)	60 s	×30	Timpe et al. 2009
Rag1midElongFb	RAG1	TGCACTGTGAYATNGGGAATGCTG	58°C (30 s)	60 s	×30	Timpe et al. 2009
ElongRag1R	RAG1	TTGACTGCCATCGCTTCCTCTCTT	58°C (30 s)	60 s	×30	Timpe et al. 2009
Rag1endElongRb	RAG1	AACTTGGACTGCCTGGCGTTCATT	58°C (30 s)	60 s	×30	Timpe et al. 2009
AL02F	EqAL02	ATGGGTCATCATCGTTATCGATATC	52°C (25 s)	45 s	×30	This study
AL02R	EqAL02	TGGTACACATTGATCCTAGATCTAG	52°C (25 s)	45 s	×30	This study
AL21F	EqAL21	TTGATCTATCGATATGCTCTAG	52°C (25 s)	45 s	×30	This study
AL21R	EqAL21	TATGCTCTCGCACAYATGATC	52°C (25 s)	45 s	×30	This study
AL51F	EqAL51	TGTCGACACATCAATGGGTGCAC	52°C (25 s)	45 s	×30	This study
AL51R	EqAL51	CACTAGACTAGCATAAATGCAGT	52°C (25 s)	45 s	×30	This study

* Internal primers.

MATERIALS AND METHODS

Molecular Sampling

We collected specimens from throughout the range of the *E. quadridigitata* complex ($n = 64$) and supplemented our sampling with loans from private individuals ($n = 42$), the Texas Cooperative Wildlife Collection Division of Herpetology ($n = 3$), and from the Louisiana State University Collection of Genetic Resources ($n = 5$) for a total of 114 individuals from 64 localities. Sample sizes ranged from one to eight individuals per locality. These *E. quadridigitata* complex samples represented *E. chamberlaini* ($n = 5$), *E. quadridigitata* ($n = 79$), the western clade ($n = 13$), the steephead/ravine clade ($n = 10$), and the hillside seepage clade ($n = 7$). The sequence from an additional sample of *E. quadridigitata* was downloaded from GenBank.

We included 34 individuals from 10 other species of the genus *Eurycea* in our phylogenetic analyses. We either collected these samples for this study ($n = 9$) or downloaded sequences from GenBank ($n = 25$), including 23 individuals from a phylogeographic study of the *E. bislineata* complex (Kozak et al. 2006). Outgroups consisted of one member from each of the remaining Spelerpini genera: *Urspelerpes brucei* (this study) and *Pseudotriton montanus*, *Gyrinophilus porphyriticus*, and *Stereochilus marginatus* (GenBank).

Tissue samples consisted of either liver or tail tips preserved in 95% ethanol and/or stored at –80°C. Voucher specimens were set in 10% formalin and stored in 70% ethanol. All museum acronyms follow Sabaj Pérez (2013) and all coordinates were taken in degree decimals in the WGS84 datum. All live animals collected for this study were handled under Florida State University IACUC protocol numbers 0905 and 1014 and collecting permits.

DNA Extraction, Amplification, and Sequencing

Genomic DNA was extracted using the hot phenol-chloroform-isoamyl alcohol/chloroform-isoamyl alcohol method (Sambrook and Russell 2001). We visualized extracts on agarose gels, and DNA concentration was quantified using a Nanodrop ND-1000 Spectrophotometer (NanoDrop, Wilmington, DE, USA) or an Invitrogen Qubit Fluorometer (Life Technologies Corporation, Carlsbad, CA, USA).

Polymerase chain reaction (PCR) was performed using the following reagents and concentrations: 13.3 µL distilled water, 5 µL 5X Colorless GoTaq Reaction Buffer, 1.5 µL $MgCl_2$ (25 mM), 1.5 µL dNTPs (2.5 mM), 0.2 µL GoTaq (5 u/µL), 0.5 µL bovine serum albumin (10 mg/ml), 1.0 µL of each primer (10 ng/µL). We amplified a 713-base pair (bp) fragment of the mitochondrial cytochrome b (CytB), a 1728-bp section of the mitochondrial genome consisting of the tRNA-Met, the entire NADH dehydrogenase subunit 2 gene, tRNA-Trp, tRNA-Ala, tRNA-Asn, the origin for light-strand replication (OLrep), tRNA-Cys, tRNA-Tyr, and part of the cytochrome oxidase subunit 1 gene (ND2/CO1/tRNAs), and a 1146-bp fragment of the nuclear recombination activating gene 1 (RAG1). Additionally, we developed three anonymous nuclear loci (ANL) using the method of Noonan and Yoder (2009). The 405-bp anonymous Locus 2 (EqAL02), the 405-bp anonymous Locus 21 (EqAL21), and the 231-bp anonymous Locus 51 (EqAL51), combined with the other three loci, represented a total of 4628 bp of sequence data.

We performed all amplifications using the primers and thermal cycler programs listed in Table 1. We used negative and positive controls for the PCR amplifications. Amplification products were purified enzymatically with Affymetrix-USB ExoSAP-IT PCR Product Clean-up kits (USB Corporation, Cleveland, OH, USA). We performed sequencing reactions at the University of Mississippi using an Applied Biosystems 3130xl Genetic Analyzer with capillary electrophoresis (Applied Biosystems Inc., Foster City, CA, USA) or at the DNA Analysis Facility at Yale University using an Applied Biosystems 3730xl Genetic Analyzer (Applied Biosystems, Inc.). We sequenced PCR products in both directions using the amplifying primers and internal sequencing primers in Table 1. Anonymous loci and some internal sequencing primers were designed using the program Geneious v5.5.7 (Kearse et al. 2012). We deposited all sequences in GenBank (see Supplemental Table S1).

We aligned and edited sequences using Geneious v5.5.7. We used the Geneious alignment algorithm for initial alignment and then adjusted manually. We translated all six sequence-reading frames into amino acids to check for stop codons and to verify the alignment. We checked

mitochondrial sequences for redundancy using Collapse v1.2 (Posada 2004) and removed redundant haplotypes. We phased the nuclear data using PHASE v2.1.1 (Stephens et al. 2001; Stephens and Scheet 2005), as implemented in DnaSP v5.10.1 (Librado and Rozas 2009), and used the most-probable alleles in the analyses. For comparative purposes, we trimmed alignments so that all individuals were represented by the same nucleotide positions and scored autapomorphies for each species from the variable sites (see alignment files in Supplemental Material).

Mitochondrial Phylogenetic Reconstruction

We first carried out a phylogenetic reconstruction using maximum parsimony (MP), maximum likelihood (ML), and Bayesian inference (BI) on the 1728-bp mitochondrial fragment consisting of ND2/CO1/tRNAs. We ran an MP and an unconstrained ML analysis using PAUP* v4.0b10 (Swofford 2003). We also conducted a heuristic search with 1000 stepwise random addition sequence replicates and using the tree bisection-reconnection branch swapping method for the MP analysis. We weighed substitutions equally and treated gaps as missing data. Using these same parameters, we conducted 860 bootstrap pseudoreplicates with 100 random addition replicates. We used AIC as implemented in jModelTest v2.1.1 (Guindon and Gascuel 2003; Darriba et al. 2012) to determine that GTR+I+Γ was the most appropriate model of evolution for the ML and BI analyses, consistent with other studies of plethodontid salamanders using these markers (Kozak et al. 2005, 2006; Wiens et al. 2006; Vieites et al. 2007). We then performed a heuristic search using 1000 stepwise random addition sequence replicates. In addition, we ran a partitioned ML analysis using RAxML v7.2.8 (Stamatakis 2006). We divided the data into eight partitions, 5′ to 3′, in the following manner: tRNA-Met, ND2 by codon position, remaining tRNAs and OLrep, and CO1 by codon position. RAxML only allows GTR enforced with the addition of Γ-distributed rate heterogeneity (GTRGAMMA), so we applied this model to each partition, using 100 stepwise random addition sequence replicates. In addition, support was measured using 1000 bootstrap pseudoreplicates in RAxML v7.2.8.

The Bayesian analysis was conducted using MrBayes v3.1.2 (Huelsenbeck and Ronquist 2001; Ronquist and Huelsenbeck 2003). The same partitions used in the ML run were used for the Bayesian analysis, and an unlinked GTR+I+Γ model was applied to all partitions. We performed two runs, utilizing six chains each (five heated and one cold), for 5×10^7 generations, sampling every 1000 generations. In addition to the average standard deviation of split frequencies, we checked for convergence of the runs using the programs AWTY (Nylander et al. 2008) and Tracer (Rambaut et al. 2014), then used Tracer to check for stationarity and determine burn-in ($= 5 \times 10^6$).

Species Tree Estimation

We subsampled 50 individuals from each of the five major clades in the ND2/CO1/tRNAs mitochondrial analysis. We estimated the species tree using 3888 bp of sequence (CytB [713 bp], ND2 [988 bp], RAG1 [1146 bp], EqAL02 [405 bp], EqAL21 [405 bp], and EqAL51 [231 bp]), population designations using the mitochondrial clades, and the multilocus Bayesian model implemented in the program *BEAST v1.7.4 (Heled and Drummond 2010), which integrates over uncertainty in the gene trees, the coalescent, and models of nucleotide evolution. We used the phased nuclear alleles in combination with the mitochondrial haplotypes. We unlinked the nucleotide substitution and clock models for all six loci and the tree model for the four nuclear loci, leaving the mitochondrial loci tree model linked. We partitioned the data by codon position and used uniform priors at each position. An uncorrelated lognormal relaxed clock model was used for each data partition. We set all tree priors to Yule process and utilized a random starting tree. We then performed two independent analyses, each for 2.5×10^8 generations and sampled every 2.5×10^3 generations. We combined the resultant data sets using LogCombiner v1.7.4 (Drummond and Rambaut 2007) and checked for convergence using AWTY (Nylander et al. 2008) and Tracer (Rambaut et al. 2014). Stationarity was checked using Tracer and we discarded the first 20,000 trees as burn-in.

Bayesian Species Delimitation

We used a modified version of the Bayesian species delimitation method of Leaché and Fujita (2010), choosing our populations based on the deep clades recovered in the mitochondrial phylogenetic analysis rather than using a model-based cluster analysis of allele frequencies. We used the program Bayesian Phylogenetics and Phylogeography (Rannala and Yang 2003; Yang and Rannala 2010) to conduct the species delimitation analysis. The method implemented takes into account both the species phylogeny and issues of lineage sorting due to ancestral polymorphism. We used the species tree from our *BEAST analysis as the guide tree with the default species model prior (uniform rooted trees). In order to examine the robustness of our results, we employed gamma priors with three combinations of parameter values for the population sizes (θs) and root age of the species tree (τ_0): (1) $\theta = G(1, 10)$, $\tau_0 = G(1, 10)$; (2) $\theta = G(2, 2000)$, $\tau_0 = G(2, 2000)$; and (3) $\theta = G(1, 10)$, $\tau_0 = G(2, 2000)$. Other divergence time parameters were assigned a Dirichlet prior (Yang and Rannala 2010; Equation 2). The latter combination of parameter values (i.e., large ancestral population size and relatively shallow divergence times) is considered a conservative combination in that it should favor fewer species delimitations (Leaché and Fujita 2010; Yang and Rannala 2010). In order to insure proper mixing of the reverse jump Markov chain Monte Carlo (rjMCMC), we ran one analysis with each species delimitation model as the starting tree ($n = 5$) and ran at least one analysis utilizing each of the rjMCMC algorithms (Yang and Rannala 2010; Equations 3 and 4 and Equations 6 and 7, respectively). We ran each analysis for 50,000 generations with a burn-in of 5000, which has been shown to be long enough to ensure convergence in many large datasets (Yang and Rannala 2010).

Morphological Data

We collected data for 13 morphological characters from 219 preserved salamanders. This total was composed of specimens used in the molecular analyses and museums specimens collected from the exact same locality as animals used in the molecular analyses. Sex can be difficult to ascertain in most salamanders due to a lack of obvious sexual dimorphism (Petranka 1998). We did not dissect specimens

to determine sex because specimens are small and we did not want to risk permanent damage or destruction. Whenever possible, we sexed animals based on the presence of cirri (secondary sexual character on the snout of males) or when ova could be detected through the thin abdominal wall of a female. Measurements consisted of (1) snout–vent length (SVL = distance from tip of snout to posterior edge of cloaca); (2) tail length (TL = distance from posterior edge of cloaca to tip of tail); (3) total length (L = SVL + TL); (4) tail height (TH = dorsal–ventral distance immediately behind cloaca); (5) tail width (TW = lateral distance immediately behind cloaca); (6) hindlimb length (HLL = outstretched distance between the limb insertion and longest toe); (7) forelimb length (FLL = outstretched distance between the limb insertion and longest toe); (8) head length (HL = midline distance between tip of snout and gular fold); (9) head width (HW = distance at widest point on head); (10) head depth (HD = dorsal–ventral distance in front of gular fold); (11) canthus length (CL = distance between anterior corner of eye and midline tip of snout); (12) interocular distance (IO = distance between anterior corners of eyes); and (13) ocular distance (OD = distance between anterior and posterior corners of eye). We took all limb measurements on the left side. We noted when tails had been broken or regenerated. All measurements were taken to the nearest 0.1 mm using 150-mm digital calipers.

Morphological Analyses

We conducted all analyses using the R statistical package v3.3.1 (R Core Team 2016). To allow for relative comparisons between taxa, we first standardized the TH, TW, HL, FLL, HL, HW, HD, CL, IO, and OD measurements for each specimen by dividing each measurement by its respective SVL. We also calculated several other ratios for comparative purposes, including SVL/L, TL/L, HW/HL, CL/HL, IO/HW, OD/CL, and FLL/HLL. We then calculated the means and standard deviations on all character measurements and ratios for each species.

We conducted a principal components analysis (PCA) on the covariance matrix of the morphological traits in order to obtain standardized principal components (PC) using the Rcmdr package (Fox 2005). When variable loadings of PC1 are of similar magnitude and direction, this is often interpreted as being a strong correlation between size and other morphometric variables (Jolicoeur 1963). Subsequent PC axes are then interpreted as estimates of the contribution of other morphological traits to body shape. In order to explore the effect of these traits on shape among the five lineages, we first natural log transformed each of 12 measurements (we did not use L) and then subtracted each log transformed measurement from its respective log transformed SVL. This method removes the size effect before the PCA is performed, resulting in the interpretation of all PC axes as the contribution of the morphological traits to shape among the species (Mosimann and James 1979).

We checked for normality of our morphological traits with histograms, quantile–quantile probability plots, and the Shapiro-Wilk test using the Rcmdr package. We then performed a series of Kruskal-Wallis tests and Dunn's tests on the standardized ratios of measurements, PC1, and PC2 using the dunn.test package (Dinno 2016). This package first performs a Kruskal-Wallis test, a nonparametric version of the one-way analysis of variance (ANOVA) that uses rank sums to test the null hypothesis that the medians of the groups are equal (Kruskal and Wallis 1952). If the null hypothesis is rejected, this package then performs Dunn's test, a post hoc pairwise rank sum test. Unlike the Mann-Whitney *U*-test (Wilcoxon rank-sum test), Dunn's test uses the same ranks and pooled variance from the Kruskal-Wallis test (Dunn 1961). We used the holm function to apply the Holm-Bonferroni method of correcting *P*-values because Dunn's test performs several simultaneous pairwise comparisons (Holm 1979).

Results

Phylogenetic Analysis

We used a total of 150 sequences representing 16 species of plethodontid salamanders from the Spelerpini in the ND2/CO1/tRNA alignment. We detected no premature stop codons in the ND2 or CO1 genes, strongly suggesting that the amplicons were indeed mitochondrial in nature and not the result of a duplication event inserted into the nuclear genome (Zhang and Hewitt 1996). The resulting alignment was unambiguous except for a series of eight indels with the following locations: 9 bps between ND2 and tRNA-Trp, 16 bps between tRNA-Trp and tRNA-Ala, 6 bps between tRNA-Ala and tRNA-Asn, 4 bps within tRNA-Asn, 2 bps within OLrep, 2 bps within OLrep, 1 bp between tRNA-Cys and tRNA-Tyr, and 6 bps within tRNA-Tyr. We excluded these ambiguous indels from all analyses. The Collapse run found 17 redundant haplotypes. In each case, the redundant haplotype was from the same geographic locality as its duplicate, so the shorter of the two sequences was removed from the alignment. This resulted in a 1728-bp alignment of 133 sequences used in the phylogenetic analyses. The AIC results from the jModelTest run suggested GTR+I+Γ was the best model of nucleotide evolution. The ML tree from the PAUP* analysis is reported (Fig. 2) with bootstrap support values from the MP and RAxML analyses and posterior probabilities from the BI (MP/RAxML/BI). All four phylogenetic analyses (MP, ML, RAxML, and BI) reconstructed nearly identical trees (the partitioned and unpartitioned ML trees were identical), with differences detailed herein.

The monotypic genus *Urspelerpes* was the sister taxon to a strongly supported, monophyletic *Eurycea*. All three analyses strongly supported the monophyly of the Ozark *Eurycea* complex, the *E. longicauda* complex, and the *E. bislineata* complex. Within the *E. bislineata* complex, the 23 GenBank samples had the exact same relationship as reported in Kozak et al. (2006). There was poor support for the monophyly of the *E. quadridigitata* complex in all three analyses, with the proposed relationships to other *Eurycea* varying. The MP tree consisted of a polytomy made up of the Ozark complex, the *E. lucifuga* complex, the *E. bislineata* complex, and three well supported clades of the *E. quadridigitata* complex: a clade containing *E. quadridigitata* sensu stricto + *E. chamberlaini* + the steephead/ravine clade, the hillside seepage clade, and the western clade (Fig. 2).

The ML and BI trees were similar to the MP tree in these relationships, with a few exceptions. In these trees, *E. quadridigitata* sensu stricto, *E. chamberlaini*, the steephead/ravine clade, and the hillside seepage clade formed a strongly

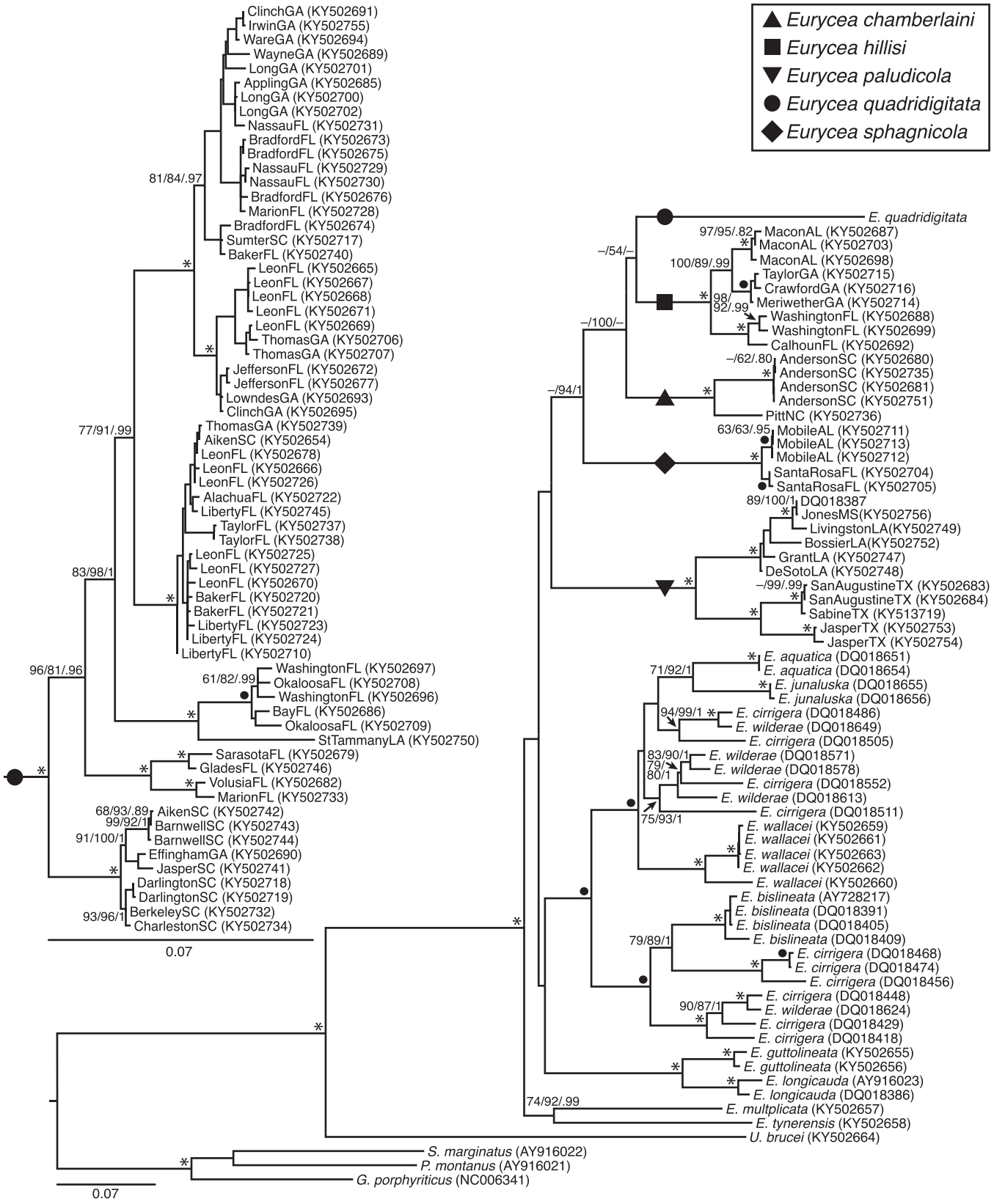

FIG. 2.—Maximum likelihood phylogram of the mitochondrial ND2, tRNAs, and partial CO1 genes. Support values are reported on nodes as maximum parsimony bootstrap/RAxML bootstrap/Bayesian posterior probabilities. Nodes denoted with solid circles or asterisks represent clades with support values ≥95/95/.95 or ≥99/99/.99, respectively. Some support values for recent nodes were not shown for clarity. Symbols for clade designations correspond to those in Fig. 1.

supported monophyletic group (Fig. 2). However, both trees showed weak support for a monophyletic *E. quadridigitata* complex, with the western clade as the sister group to other *Eurycea* complexes, rendering *E. quadridigitata* paraphyletic.

Nearly all other deep clades and relationships in the *E. quadridigitata* complex were strongly supported, the exception being the placement of the strongly supported *E. chamberlaini* clade. In the MP and BI trees, *E. chamberlaini* was sister to *E. quadridigitata* sensu stricto, though this relationship was weakly supported (MP bootstrap = 56, BI posterior probability = 0.33). In both trees, the steephead/ravine clade was sister to *E. chamberlaini* + *E. quadridigitata* sensu stricto. In all analyses, the western clade was strongly supported as being monophyletic, regardless of its position in the phylogeny.

Species Tree and Delimitation

The AIC results from the jModelTest runs indicated the following nucleotide substitution models as the best fit: TPM1uf+I+Γ (AL02), TPM3uf+I (AL21), TrNef+I (AL51), TPM3+I+Γ (RAG1), GTR+I+Γ (CytB), and TIM1+I+Γ (ND2). Due to restrictions in available nucleotide substitution models in *BEAST, we implemented the next-most complex model for each locus, resulting in the following models: TrNef+I with equal rates (AL51), GTR+I with equal rates (AL21), and GTR+I+Γ (AL02, RAG1, CytB, and ND2).

The individual gene trees from our *BEAST analysis were congruent in most major aspects (see Supplemental Fig. S1). In all five trees, the western clade and hillside seepage clades formed well-supported clades with posterior probabilities (PP) = 0.96–1.0. In two gene trees (RAG1 and mtDNA), the western clade was the sister clade to the rest of the tree, but in the AL02 tree the hillside seepage clade was the sister clade to the rest of the tree. In the AL21 (PP = 0.88) and AL51 (PP = 0.86), the western clade and hillside seepage clade formed a clade that was sister to the rest of the tree. *Eurycea quadridigitata* sensu stricto, the steephead/ravine clade, and *E. chamberlaini* formed a clade with PP = 1.0 in all five gene trees. In the RAG1 and mtDNA trees, the steephead/ravine clade (PP = 0.98 and 1.0, respectively) and western clade (PP = 0.64 and 1.0, respectively) were monophyletic but did not form a clade in the anonymous loci. The remaining relationships in *E. quadridigitata* sensu stricto, the steephead/ravine clade, and the western clade were in conflict between most trees and showed moderate (RAG1) to poor (anonymous loci) support, with the mtDNA tree being the exception. This is expected, given the smaller effective population size and faster coalescence of the haploid mitochondria.

The species tree from the *BEAST run is shown in Fig. 3. The root connecting all five populations was supported with a PP of 1.0. The western clade was sister to the other four clades. The remaining four formed a clade (PP = 0.85) with the hillside seepage clade sister to the remaining three clades. The divergence between the hillside seepage clade and these clades was relatively deep in the tree. The next clade was supported with a PP of 1.0 and was much shallower than the previous node. It was composed of a clade containing the steephead/ravine clade and *E. chamberlaini* (PP 0.45), which was sister to *E. quadridigitata* sensu stricto.

The results from the BPP species delimitation analysis (Fig. 3) provided strong support for the five-species model (1111) across all combinations of starting trees and parameters, with the exception of a single run with large θ (G[1, 10]) and large τ_0 (G[1, 10]) that used the 1100 model as the starting tree. In this analysis, the 1100 model was selected with a speciation probability of 1.0 for both nodes, supporting a three-species delimitation.

Morphological Analyses

The ranges, means, and standard deviations of the 17 morphometric ratios are reported in Table 2 (for raw measurements see Supplemental Table S2). We failed to reject normality for SVL, TL, HLL, FLL, and HL, but normality was rejected for the remaining traits: TW, TH, HW, HD, CL, IO, and OD.

Principal component loadings from the first six axes of the PCA on the covariance matrix of morphological traits are reported in Table 3. Because we corrected for size before we ran the PCA, we interpret the axes as the effect of the traits on shape. The first PC explained 45% of the total variation with the PC loadings all positive but variable in magnitude, with the highest loadings for TW, TH, HD, IO, OD, HL, and HW. The second PC explained an additional 22% of the variation, with high positive loadings on TW and TH but high negative loadings on IO, FLL, HL, and HLL. The next 7% of the variation was explained by PC3, having large positive loadings on CL, TH, HLL, and FLL but large negative loadings on HD and IO. The fourth PC explained an additional 6% of the variation, with the largest positive loadings coming from FLL and HLL and the largest negative loadings from CL and IO. Principal component five explains another 6% of the variation, with the largest positive loadings on HD and TH and largest negative loadings on TW, IO, and FLL. The sixth PC axis explains 5% of the variation, with a large positive loading on TH and IO and large negative loadings on OD, HD, TW, CL. The remaining variance is explained by PC7–PC10 (see Supplemental Table S3). A plot of PC1 vs. PC2 reveals that elements of the tail (TH and TW) and head (particularly depth and width) are inversely related and explain much of the observed variation (Fig. 4). The second PC reveals an inverse relationship between these same tail characters and limb lengths.

With more than half the traits not being normally distributed, we opted to analyze all traits under the Kruskal-Wallis test. This is a less powerful test than the one-way ANOVA and therefore a more conservative approach. In attempting to find characters that distinguish one species from another, we feel a conservative approach is a better approach. We found highly significant differences among populations for SVL/L ($H = 21.37$, df = 4, $P < 0.0001$), TW/SVL ($H = 38.42$, df = 4, $P < 0.0001$), TH/SVL ($H = 29.58$, df = 4, $P < 0.0001$), HHL/SVL ($H = 19.40$, df = 4, $P < 0.0001$), FFL/SVL ($H = 27.20$, df = 4, $P < 0.0001$), HL/SVL ($H = 79.94$, df = 4, $P < 0.0001$), HW/SVL ($H = 50.58$, df = 4, $P < 0.0001$), HD/SVL ($H = 75.94$, df = 4, $P < 0.0001$), CL/SVL ($H = 10.58$, df = 4, $P = 0.03$), IO/SVL ($H = 62.41$, df = 4, $P < 0.0001$), OD/SVL ($H = 57.62$, df = 4, $P < 0.0001$), HW/HL ($H = 42.62$, df = 4, $P < 0.0001$), CL/HL ($H = 53.84$, df = 4, $P < 0.0001$), IO/HW ($H = 23.48$, df = 4, $P < 0.0001$), and OD/CL ($H = 32.32$, df = 4, $P < 0.0001$).

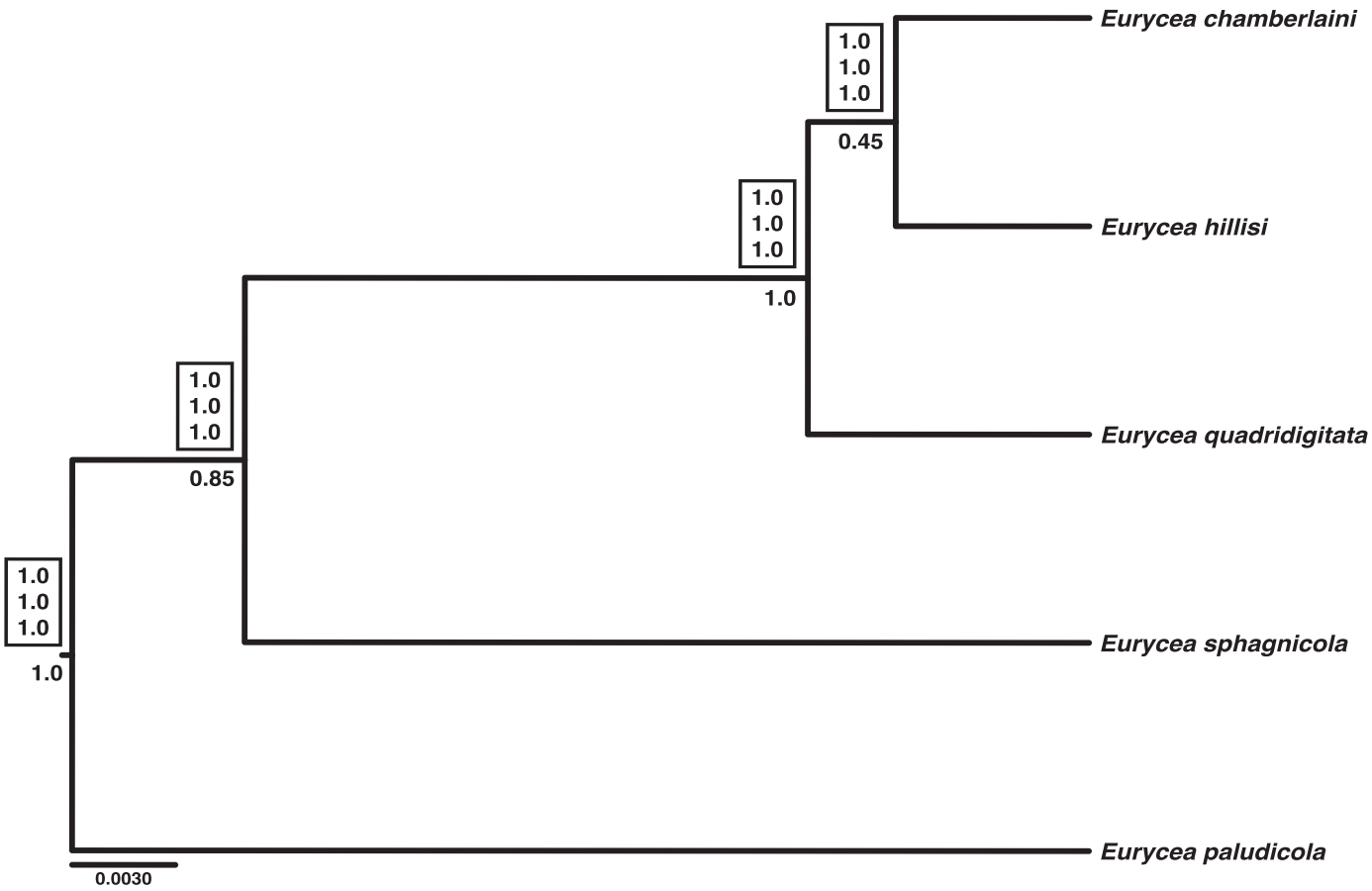

FIG. 3.— The species tree from the *BEAST analysis of four nuclear and two mitochondrial loci. Posterior probabilities from *BEAST analysis are located under respective nodes. Boxes above nodes represent species probabilities from runs with different parameter settings in the Bayesian Phylogenetics and Phylogeography species delimitation analysis: top = large ancestral population size and deep root age [$\theta = G(1, 10)$, $\tau_0 = G(1, 10)$], middle = small ancestral population size and shallow root age [$\theta = G(2, 2000)$, $\tau_0 = G(2, 2000)$], and bottom = large ancestral population size and shallow root age [$\theta = G(1, 10)$, $\tau_0 = G(2, 2000)$].

TABLE 2.—Range, mean, and standard deviation for snout–vent length (SVL) and the 17 morphometric ratios of each species in the *Eurycea quadridigitata* species complex as measured from 219 individuals. Ranges appear first followed by means ± standard deviations in parentheses. All measurements in millimeters.

	E. chamberlaini	*E. quadridigitata*	*E. paludicola*	*E. hillisi*	*E. sphagnicola*
SVL	22.6–32.3 (26.1 ± 3.7)	20.8–33.8 (26.7 ± 2.4)	22.3–37.2 (30.5 ± 4.0)	18.0–29.5 (23.8 ± 3.5)	16.4–25.7 (22.7 ± 2.2)
SVL/total length	37.4–63.9 (50.4 ± 11.6)	32.8–70.5 (43.6 ± 7.0)	37.6–61.6 (43.5 ± 5.2)	38.1–66.1 (46.6 ± 8.3)	37.7–51.0 (41.9 ± 3.7)
Tail length/total length	36.1–62.6 (49.6 ± 11.6)	29.5–67.2 (56.4 ± 7.0)	38.4–62.4 (56.5 ± 5.2)	33.9–61.9 (53.4 ± 8.3)	49.0–62.3 (58.1 ± 3.7)
Tail width/SVL	4.0–7.2 (5.8 ± 1.0)	4.2–11.2 (7.7 ± 1.3)	6.7–10.1 (8.6 ± 1.0)	5.0–9.4 (7.0 ± 1.2)	5.4–10.6 (8.5 ± 1.3)
Tail height/SVL	5.0–9.6 (7.6 ± 1.6)	6.3–13.4 (9.2 ± 1.3)	7.9–11.9 (10.2 ± 1.3)	7.8–10.5 (9.1 ± 0.8)	8.3–11.9 (10.0 ± 1.0)
Hindlimb length/SVL	24.3–31.9 (27.2 ± 2.5)	21.7–31.9 (26.7 ± 2.3)	21.2–31.4 (26.0 ± 3.0)	24.4–33.5 (27.9 ± 2.2)	24.6–35.0 (28.4 ± 2.1)
Forelimb length/SVL	19.5–27.9 (23.3 ± 3.0)	17.0–26.7 (22.3 ± 2.2)	18.5–23.8 (21.3 ± 1.5)	20.7–26.8 (23.6 ± 1.5)	19.6–29.1 (24.1 ± 2.3)
Head length/SVL	18.0–21.7 (20.2 ± 1.3)	15.4–24.4 (19.9 ± 1.6)	17.3–24.7 (19.9 ± 1.8)	18.9–24.4 (21.5 ± 1.8)	20.0–28.7 (24.0 ± 2.0)
Head width/SVL	9.6–13.7 (11.7 ± 1.3)	8.1–14.2 (12.0 ± 0.8)	10.4–14.9 (12.6 ± 1.1)	11.0–14.4 (12.9 ± 1.0)	11.5–15.5 (13.3 ± 1.0)
Head depth/SVL	5.6–8.1 (6.9 ± 0.9)	5.5–10.5 (7.1 ± 0.8)	6.1–9.9 (7.8 ± 0.8)	6.3–9.4 (8.0 ± 0.7)	7.0–12.4 (9.0 ± 1.3)
Canthus length/SVL	5.6–7.2 (6.5 ± 0.7)	4.4–7.7 (6.1 ± 0.6)	5.1–7.7 (6.6 ± 0.8)	5.1–7.3 (6.2 ± 0.5)	4.9–7.9 (6.3 ± 0.7)
Interocular distance/SVL	5.1–7.1 (6.0 ± 0.7)	3.9–7.4 (5.5 ± 0.6)	5.0–8.0 (6.0 ± 0.7)	5.1–9.4 (6.5 ± 1.0)	5.0–9.8 (6.8 ± 1.1)
Ocular diameter/SVL	4.6–5.8 (5.2 ± 0.4)	4.1–6.7 (5.3 ± 0.5)	4.3–7.2 (5.7 ± 0.7)	5.1–6.7 (5.7 ± 0.5)	4.9–8.5 (6.3 ± 0.7)
Head width/head length	53.4–63.3 (57.6 ± 3.3)	45.5–77.5 (60.6 ± 5.5)	57.9–70.9 (63.3 ± 4.0)	56.7–66.0 (60.3 ± 2.7)	41.8–64.7 (55.5 ± 3.9)
Canthus length/head length	29.8–34.0 (32.3 ± 1.5)	23.2–40.5 (30.7 ± 3.2)	27.3–36.1 (32.9 ± 2.6)	22.6–34.0 (29.1 ± 3.1)	20.7–34.5 (26.4 ± 3.4)
Interocular distance/head width	44.8–60.0 (51.9 ± 5.7)	32.4–61.9 (46.5 ± 5.2)	41.2–57.9 (48.0 ± 4.0)	40.4–71.0 (50.5 ± 7.2)	41.4–64.0 (51.4 ± 5.7)
Ocular diameter/canthus length	70.6–88.9 (80.6 ± 7.7)	64.7–127.3 (88.1 ± 10.0)	70.0–100.0 (87.5 ± 10.2)	72.2–108.3 (91.8 ± 9.9)	75.0–127.3 (100.6 ± 13.0)
Forelimb length/hindlimb length	80.2–90.8 (85.5 ± 4.4)	67.2–98.6 (83.6 ± 7.0)	72.4–100.0 (83.0 ± 9.2)	76.0–98.5 (84.9 ± 6.4)	74.2–97.9 (84.7 ± 5.1)

TABLE 3.—Principal component (PC) loadings of the first six axes from the PC analysis of 10 traits from 219 specimens in the *Eurycea quadridigitata* complex. Values in parentheses represent the proportional contribution to each principal component.

Variables	PC1	PC2	PC3	PC4	PC5	PC6
Canthus length	0.134 (0.047)	−0.182 (0.065)	0.673 (0.268)	−0.505 (0.216)	0.159 (0.061)	−0.231 (0.092)
Forelimb length	0.095 (0.034)	−0.344 (0.012)	0.227 (0.091)	0.562 (0.240)	−0.220 (0.084)	0.122 (0.049)
Head depth	0.451 (0.159)	−0.068 (0.024)	−0.519 (0.207)	0.091 (0.039)	0.425 (0.163)	−0.259 (0.103)
Head length	0.260 (0.092)	−0.296 (0.106)	−0.035 (0.014)	−0.046 (0.014)	−0.003 (0.001)	−0.111 (0.044)
Head width	0.236 (0.083)	−0.124 (0.044)	−0.038 (0.015)	0.009 (0.015)	0.187 (0.071)	−0.003 (0.001)
Hindlimb length	0.077 (0.027)	−0.288 (0.103)	0.243 (0.097)	0.471 (0.097)	−0.059 (0.023)	0.043 (0.017)
Interocular distance	0.358 (0.126)	−0.401 (0.143)	−0.247 (0.098)	−0.421 (0.098)	−0.480 (0.184)	0.427 (0.170)
Ocular distance	0.335 (0.118)	−0.187 (0.067)	0.156 (0.062)	0.079 (0.062)	0.112 (0.043)	−0.382 (0.152)
Tail height	0.390 (0.137)	0.316 (0.112)	0.256 (0.102)	0.068 (0.102)	0.428 (0.164)	0.677 (0.270)
Tail width	0.498 (0.176)	0.602 (0.214)	0.115 (0.046)	0.091 (0.046)	−0.529 (0.203)	−0.254 (0.101)
Variances	0.071	0.034	0.011	0.010	0.009	0.007
Standard deviation	0.266	0.184	0.105	0.098	0.095	0.086
Proportion of total variance explained	0.451	0.217	0.070	0.061	0.058	0.047

Only TL/L and FFL/HHL were not significant among populations.

The significant results of the post hoc Dunn's tests for the standardized ratios, PC1, and PC2 are reported in Table 4. *Eurycea quadridigitata* differed from *E. chamberlaini* in SVL/L, TW/SVL, and PC2. The characters TW/SVL, TH/SVL, HD/SVL, IO/SVL, CL/HL, and PC1 separated *E. quadridigitata* from the western clade animals. The characters separating the steephead/ravine clade animals from *E. quadridigitata* were all head morphologies and included HL/

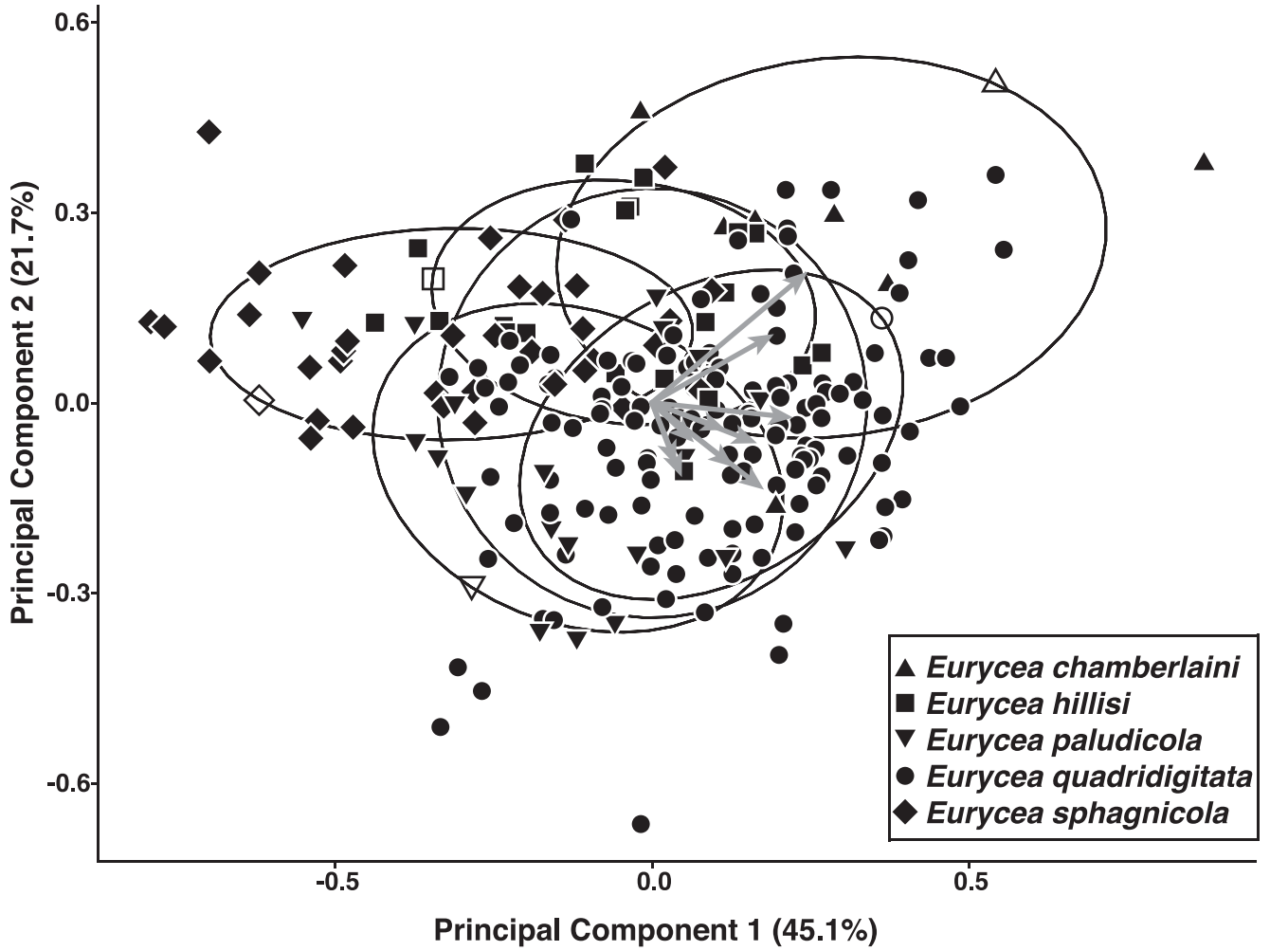

FIG. 4.—Plot of principal component 1 (PC1) vs. PC2 from principal component analysis using 10 characters from 219 individuals of the *Eurycea quadridigitata* complex. Aspects of the head and tail morphology explain most of the variance observed in PC1 whereas an inverse relationship between limb length and tail morphology explain most of the variance in PC2. Gray arrows clockwise from top represent tail width, tail height, head depth, head width, ocular diameter, head length, interocular distance, canthus length, hindlimb length, and forelimb length. Symbols correspond to those in Figs. 1 and 2. Open symbols indicate the appropriate 95% confidence ellipse for each species.

TABLE 4.—Results of the Dunn's tests from the measurement ratios, principal component 1 (PC1), and PC2 of the 219 specimens in the *Eurycea quadridigitata* complex. This post hoc test is a multiple pairwise comparison for each ratio among all five species following a significant Kruskal-Wallis test. We Holm-Bonferroni corrected all probabilities to account for the family-wise error rate. For clarity and brevity, only the significant results are shown (ns = nonsignificant). Probabilities follow Dunn's *z*-statistic. SVL = snout–vent length.

	Eurycea quadridigitata	*Eurycea hillisi*	*Eurycea sphagnicola*	*Eurycea paludicola*
Eurycea hillisi				
Head length/SVL	−3.099 ($P = 0.006$)			
Head width/SVL	−3.698 ($P = 0.001$)			
Head depth/SVL	−4.362 ($P < 0.001$)			
Interocular distance/SVL	−4.647 ($P < 0.001$)			
Principal component 2	5.146 ($P < 0.001$)			
Eurycea sphagnicola				
Tail width/SVL	−3.366 ($P = 0.002$)	−3.852 ($P < 0.001$)		
Tail height/SVL	−3.750 ($P < 0.001$)	−2.812 ($P = 0.015$)		
Hindlimb length/SVL	−3.841 ($P < 0.001$)	ns		
Forelimb length/SVL	−3.852 ($P < 0.001$)	ns		
Head length/SVL	−8.612 ($P < 0.001$)	−3.127 ($P = 0.006$)		
Head width/SVL	−6.318 ($P < 0.001$)	ns		
Head depth/SVL	−7.838 ($P < 0.001$)	ns		
Interocular distance/SVL	−6.894 (P < 0.001)	ns		
Ocular diameter/SVL	−7.294 ($P < 0.001$)	−2.818 ($P = 0.017$)		
Head width/head length	5.396 ($P < 0.001$)	3.579 ($P = 0.001$)		
Canthus length/head length	5.789 ($P < 0.001$)	ns		
Interocular distance/head width	−4.161 ($P < 0.001$)	ns		
Ocular diameter/canthus length	−5.048 ($P < 0.001$)	ns		
Principal component 1	−7.498 ($P < 0.001$)	−2.999 ($P = 0.008$)		
Principal component 2	5.207 ($P < 0.001$)	ns		
Eurycea paludicola				
Tail width/SVL	−3.072 ($P = 0.004$)	−3.728 ($P < 0.001$)	ns	
Tail height/SVL	−3.185 ($P = 0.005$)	−2.669 ($P = 0.019$)	ns	
Hindlimb length/SVL	ns	ns	3.288 ($P = 0.005$)	
Forelimb length/SVL	ns	3.425 ($P = 0.003$)	4.330 ($P < 0.001$)	
Head length/SVL	ns	ns	5.811 ($P < 0.001$)	
Head depth/SVL	−3.313 ($P = 0.003$)	ns	ns	
Interocular distance/SVL	−2.791 ($P = 0.021$)	ns	ns	
Ocular diameter/SVL	ns	ns	2.844 ($P = 0.018$)	
Head width/head length	ns	ns	−5.710 ($P < 0.001$)	
Canthus length/head length	−2.902 ($P = 0.011$)	−3.401 ($P = 0.002$)	−6.383 ($P < 0.001$)	
Ocular diameter/canthus length	ns	ns	3.502 ($P = 0.002$)	
Principal component 1	−3.617 ($P = 0.001$)	ns	ns	
Principal component 2	ns	−4.654 ($P < 0.001$)	−4.357 ($P < 0.001$)	
Eurycea chamberlaini				
SVL/total length	−4.432 ($P < 0.001$)	−3.779 ($P < 0.001$)	−3.664 ($P < 0.001$)	−4.278 ($P < 0.001$)
Tail width/SVL	3.252 ($P = 0.003$)	ns	4.578 ($P < 0.001$)	4.545 ($P < 0.001$)
Tail height/SVL	ns	ns	3.749 ($P = 0.001$)	3.663 ($P = 0.001$)
Head length/SVL	ns	ns	3.423 ($P = 0.003$)	ns
Head depth/SVL	ns	ns	3.756 ($P = 0.001$)	ns
Ocular diameter/SVL	ns	ns	3.682 ($P = 0.001$)	ns
Head width/head length	ns	ns	ns	2.831 ($P = 0.016$)
Canthus length/head length	ns	ns	−4.105 ($P < 0.001$)	ns
Ocular diameter/canthus length	ns	ns	3.994 ($P < 0.001$)	ns
Principal component 1	ns	2.586 ($P = 0.024$)	4.774 ($P < 0.001$)	3.264 ($P = 0.004$)
Principal component 2	3.734 ($P = 0.001$)	ns	ns	3.840 ($P < 0.001$)

SVL, HW/SVL, HD/SVL, IO/SVL, and PC2. Nearly every character we analyzed differed significantly between the hillside seepage clade animals and *E. quadridigitata* (TW/SVL, TH/SVL, HLL/SVL, FLL/SVL, HL/SVL, HW/SVL, HD/SVL, IO/SVL, OD/SVL, HW/HL, CL/HL, IO/HW, OD/CL, PC1, and PC2). The western clade animals differed from *E. chamberlaini* in SVL/L, TW/SVL, TH/SVL, HW/HL, PC1, and PC2. The western clade animals and the steephead/ravine animals differed in TW/SVL, TH/SVL, FLL/SVL, CL/HL, and PC2. Similar to *E. quadridigitata*, the western clade animals were significantly different from the hillside seepage clade animals in a number of characters including HLL/SVL, FLL/SVL, HL/SVL, OD/SVL, HW/HL, CL/HL, OD/CL, and PC2. The hillside seepage clade also differed from *E. chamberlaini* in a number of characters (SVL/L, TW/SVL, TH/SVL, HL/SVL, HD/SVL, OD/SVL, CL/HL, OD/CL, and PC1), but less characters differentiated the hillside seepage clade from the steephead/ravine clade (SVL/L, TW/SVL, TH/SVL, HW/HL, PC1, and PC2). The fewest morphological characters that separated any two taxa were between *E. chamberlaini* and the steephead/ravine clade animals, which only differed in SVL/L and PC1.

Molecular Data

The total number of variable sites and molecular autapomorphies for all five species are listed in Table 5. These molecular characters were based off of the six genes with final alignment sizes after removal of redundant haplotypes of 713 bp (CytB) for 44 individuals, 543 bp (ND2 and tRNA) for 94 individuals, 506 bp (RAG1) for 78

TABLE 5.—Genetically variable sites and autapomorphies from six genes for each species in the *Eurycea quadridigitata* complex. Autapomorphies are in bold. For the nuclear genes (RAG1, AL02, AL21, and AL51), position number represents the site position in our alignments. For the mitochondrial genes (CytB and ND2), we used the complete mitochondrial genome of *E. bislineata* (GenBank accession number AY728217) in our alignment so that position number represents the site position in the mitochondrial genome. Multiple character states separated by a comma (e.g., A, G) represent variation at a site within a species. Character states having a forward slash (e.g., A/G) represent a heterozygous state.

Gene	Position	*E. quadridigitata*	*E. chamberlaini*	*E. hillisi*	*E. sphagnicola*	*E. paludicola*
CytB	14091	A	A	A	**G**	A
CytB	14094	T	T	T	**C**	T
CytB	14127	C	C, T	T	C	**A**
CytB	14133	A	A	A	**G**	A, T
CytB	14145	C, T	T	T	**A**	T
CytB	14163	A, G	A	A	**C**	A, G
CytB	14166	T	T	C	**A**	C, T
CytB	14241	C, A	C	C	**T**	C
CytB	14250	C	C	C	C	**T**
CytB	14259	A	A, G	A	**T**	A
CytB	14274	A	A	A	A	**T**
CytB	14328	C, T	C	C, T	C	**A, G**
CytB	14349	T	T	T	T	**G**
CytB	14416	C	**T**	C	C	C
CytB	14454	T	**C**	T	T	T
CytB	14493	T	T	T	T	**A, C**
CytB	14538	**C**	A	A	A	A
CytB	14544	T	T	T	**C**	T
CytB	14547	A	A	A	**G**	A
CytB	14588	A	A	A	**G**	**C**
CytB	14614	**C**	T	T	T	T
CytB	14623	T	T	**C**	T	**A**
CytB	14634	**A, G**	C	C	C	C
CytB	14646	T	T	T	**A**	T
CytB	14658	T	T	T	**C**	T
CytB	14665	G	G	G	**C**	G
CytB	14702	A	A	A	**G**	A
CytB	14709	T	T	T	T	**C**
CytB	14736	C	C	**A**	T	T
CytB	14738	T	T	T	T	**A**
CytB	14746	C	C	C	C	**A**
CytB	14751	A	A	A	**T**	A
CytB	14755	A	A	A	A	**T**
CytB	14759	T	T	T	**G**	T
CytB	14767	A	A	A	A	**T**
CytB	14770	C, T	C	C, T	C	**A**
CytB	14772	A	**T**	A	A	A
CytB	14781	**C**	T	T	T	T
CytB	14782	T	T	C, T	T	**A**
CytB	14790	A	A	**T**	A	A, G
CytB	14793	A	A, G	A	A	**C**
CytB	14796	A	A, G	A, G	A	**C**
CytB	14799	A	A, G	A	A	**A**
ND2	4410	A	A, G	A, G	A	**C**
ND2	4414	T	**C**	T	T	T
ND2	4416	G	G	G	**A**	G
ND2	4419	C	C	C	C	**T**
ND2	4422	**G**	A	A	A	A
ND2	4426	**T**	A	A	**G**	A
ND2	4429	C, T	C	C	**A**	C, T
ND2	4439	A	A	A	A	**T**
ND2	4442	A	A	A	A	**C, T**
ND2	4451	C	C	C	**T**	C
ND2	4455	A, G	A	A, T	**C**	A
ND2	4457	A, G	A	A	A	**T**
ND2	4468	**G**	T	T	T	T
ND2	4483	T	T	T	**C**	T
ND2	4493	A	A	A	**G, T**	A
ND2	4494	A	A	A	A	**C, T**
ND2	4503	C	C	**T**	C	C
ND2	4506	T	T	T	**A**	T
ND2	4535	C	**T**	C	C	A, C
ND2	4542	A	A	A	**G**	A
ND2	4550	C, T	C	C, T	**G**	C
ND2	4554	T	T	T	T	**A**
ND2	4555	C	C	C	C	**T**
ND2	4561	**T**	C	C	C	C
ND2	4567	T	T	T	**C**	T
ND2	4569	A	**G**	A	A	A
ND2	4609	C	C	C	**T**	C
ND2	4610	C	C	C	**A**	**T**
ND2	4620	T	T	**C**	T	**A/G**
ND2	4634	**T**	A	A	A	A
ND2	4658	**C, T**	A	A	**G**	A
ND2	4662	A	A	A	**T**	A
ND2	4665	A	**G**	A	A	A
ND2	4670	**A**	T	T	T	C, T
ND2	4671	A, G	A	A	A	**T**
ND2	4676	C	C	C	**A**	C, T
ND2	4678	C	**T**	C	C	C
ND2	4679	T	T	T	T	**C**
ND2	4700	**C**	T	T	T	T
ND2	4712	**T**	C	C	C	C
ND2	4719	C, T	**A**	T	C	C, T
ND2	4734	A, G	A	G	G	**T**
ND2	4738	C	C	C	C	**T**
ND2	4759	C	C	C	C	**A**
ND2	4761	C, T	C	C	**A**	C
ND2	4762	T	T	T	**C**	T
ND2	4788	A, C	C	C	C	**T**
ND2	4798	C	C	C	C	**T**
ND2	4806	A	A	A	A	**C**
ND2	4837	C	C	C	C	**T**
ND2	4874	A	A	A	**G**	A
RAG1	171	G	G	G	G	**A**
RAG1	210	C	C	C	C	**T**
RAG1	258	G	**A**	G	G	G
RAG1	382	A	A	A	**T**	A
RAG1	468	G	G	G	**A**	G
AL02	27	**G**	A	A	A	A
AL02	132	T	T	T	T	**G**
AL02	318	A	A, A/G	G, A/G	G	**T**
AL02	330	**C**	G	G	G	G
AL02	364	T	T	T	T	**C**
AL02	381	C	C	C	C	**A**
AL21	8	A	A	A	A	**G**
AL21	23	T	T	T	T	**C**
AL21	28	T	T	T	**A**	T
AL21	326	G	G	G	**A**	G
AL21	347	C	C	C	**A**	**T**
AL51	31	G	G	G	**A**	G
AL51	143	T	T	T	T	**G**
AL51	228	T	T	T	T	**A**
Total Autapomorphies		**15**	**10**	**5**	**42**	**48**

individuals, 405 bp (AL02) for 49 individuals, 405 bp (AL21) for 50 individuals, and 213 bp (AL51) for 50 individuals (see alignment files in Supplemental Material). Although for any one pairwise comparison among the five taxa there exists a large number of molecular differences, each taxon has a number of autapomorphies that separate it from the other four. The greatest number of autapomorphies was found in the western clade ($n = 48$) followed closely by the hillside seepage clade ($n = 42$). Fifteen autapomorphies were present in *E. quadridigitata* sensu stricto and 10 autapomorphies were present in *E. chamberlaini*. The fewest

autapomorphies were found in the steephead/ravine clade ($n = 5$).

DISCUSSION

The results of our phylogenetic analyses agree with those of Camp et al. (2009), strongly supporting *Urspelerpes* as the sister group to *Eurycea*. There is also strong support for a monophyletic *Eurycea*; however, the basal nodes within the genus are not well supported. These analyses were unable to resolve whether the *E. quadridigitata* complex is monophyletic; however, Lamb and Beamer (2012), using four mitochondrial and two nuclear markers, found the *E. quadridigitata* complex to be paraphyletic with respect to the neotenic *Eurycea* of the Edwards Plateau. This discrepancy is probably due to the fact that we did not include any members of the *Eurycea* complex from the Edwards Plateau of Texas. Other studies using multiple markers and nearly complete sampling within the Spelerpini also found the *E. quadridigitata* complex to be paraphyletic, with the western clade animals being the sister group to the neotenic Edwards Plateau *Eurycea* clade (Bonett et al. 2014; Wray and Steppan 2016). Within the *E. quadridigitata* complex, there was strong support for many deeply divergent lineages, which is in agreement with the findings of Wray and Steppan (2016) but still somewhat unexpected given the absence of any recognized subspecies. Three of these divergences are deeper than any divergence seen within any other species or species complex within the genus (Fig. 2). This is most evident when compared with the *E. bislineata* complex, which is composed of six described species and several putative ones (Kozak et al. 2006), strongly suggesting that *E. quadridigitata* sensu lato is composed of multiple, undescribed species and confirmed by the results of our species delineation method.

Despite having been described nearly 175 yr ago, only two studies to date have found any morphological differences within *E. quadridigitata* sensu lato. Mittleman (1947) found only limited meristic differences that were later refuted by the same author (Mittleman 1967). It was not until Harrison and Guttman (2003) that a comprehensive study revealed meristic, morphometric, and allozyme differences within *E. quadridigitata* sensu lato, resulting in the description of *E. chamberlaini*. Since the description of *E. chamberlaini*, a number of molecular studies have demonstrated significant genetic variation within *E. quadridigitata* sensu lato, indicating that a number of undescribed taxa may exist (Kozak et al. 2009; Lamb and Beamer 2012; Bonett et al. 2014; Wray and Steppan 2016).

Under the general lineage concept of species (de Queiroz 1998, 2007), our results demonstrate conclusively that there are at least five species in the *E. quadridigitata* complex which can be delimited and diagnosed from one another using meristic, morphometric, molecular, and ecological criteria. Therefore, in the following accounts we (1) add additional characters to the diagnosis of *E. chamberlaini*; (2) redefine *E. quadridigitata* in the context of our results; (3) resurrect a former subspecies; (4) describe the steephead/ravine breeding clade; and (5) describe the hillside seepage breeding clade.

SPECIES DESCRIPTIONS

Eurycea chamberlaini Harrison and Guttman 2003 (Figs. 1, 5A; Tables 2, 5)

Manculus quadridigitatus quadridigitatus: Mittleman 1947:219. [in part, misidentification].

Manculus quadridigitatus: Mittleman 1967:1. [in part, misidentification].

Holotype.—An adult female (USNM 547846) from Sesquicentennial State Park, Richland County, South Carolina, collected 3 August 1974 by Julian R. Harrison.

Paratypes.—NORTH CAROLINA ($n = 35$; Note there is a discrepancy in this total number and the following number of individuals [34] in the original description): eight specimens (NCSM 14947 [$n = 5$], NCSM 17103 [$n = 3$]) from 1.5 mi SSW Wilsonville, Chatham County; one specimen (NCSM 36024) from ca. 3 mi E Tuscarora, Craven County; one specimen (NCSM 15788) from 2 mi NE Four Oaks, Johnston County; one specimen (NCSM 19159) from 2 mi NW Deep Run, Lenoir County; two specimens (NCSM 17470) from 8.25 mi SW Robbins, Moore County; two specimens (NCSM 36023) from 7 mi WSW Oriental, Pamlico County; two specimens (NCSM 17556) from 4.8 mi NNE Delway, Sampson County; three specimens (NCSM 14805) from 4 mi E Henderson, Vance County; 13 specimens (ChM CA4571–7 [JRH 3178–84], NCSM 17355, NCSM 17579 [$n = 4$], NCSM 19783) from 4.5 mi S Cary, Wake County; one specimen (NCSM 36022) from 2 mi E Holly Springs, Wake County.

SOUTH CAROLINA ($n = 15$): four specimens (ChM CA4566–9 [JRH 3286–9]) from Rainbow Bay, Savannah River Site, Barnwell County; one specimen (ChM CA4570 [JRH 3177]) from near Clemson, Pickens County; two specimens (USNM 547847–8 [JRH 2701–2]) from Sesquicentennial State Park, Richland County; eight specimens (NCSM 36021) from N edge of Sumter, Sumter County.

Referred specimens.—NORTH CAROLINA ($n = 1$): one specimen (UF178914 [KW0128]) from Greenville, Pitt County, 34.61266°N, 77.36635°W.

SOUTH CAROLINA ($n = 6$): two specimens (UF178975–6 [SREL 2218–9]) from Gum Swamp Road, Beech Island, Aiken County, 33.39680°N, 81.90150°W; one specimen (UF178913 [KW0127]) from creek crossing at SH 162, 0.33 mi W of SH 76, La France, Anderson County, 34.60595°N, 82.76982°W; two specimens (UF178850–1 [DBM 3285]) from Pendelton Swamp, S of SR S-4-115, 0.18 mi W of SH 178, Anderson County, 34.64977°N, 82.70692°W; one specimen (UF178977 [SREL 2220]) from University of South Carolina Upstate Campus, Spartanburg, Spartanburg County, 34.99520°N, 81.95559°W.

Comparisons.—Variation in the 17 ratios for the seven animals examined is listed in Table 2 (for variation in the 13 morphometric characters see Supplemental Table S2). Molecular variation for six loci is listed in Table 5. See Harrison and Guttman (2003) for additional variation. Characters separating *E. chamberlaini* from each of the other members of the species complex are listed herein, followed by character states of other species in parentheses.

The following characters were used to distinguish *E. chamberlaini* from *E. quadridigitata* in the original description (Harrison and Guttman 2003): adpressed limbs

FIG. 5.—*Eurycea quadridigitata* complex. (A) *E. chamberlaini* (KW0127), gravid female from Anderson County, SC; (B) *E. quadridigitata* (KW0004), neotype from Leon County, Florida; (C) *E. quadridigitata*, adult from Leon County, Florida; (D) *E. quadridigitata*: adult male from Liberty County, Florida; (E) *E. quadridigitata* (KW0021): adult from Berkeley County, South Carolina; (F) *E. quadridigitata* (KW0124): adult male from Charleston County, South Carolina.

relatively longer (relatively shorter); costal groove count 15–16 (17–18); average of 10 prevomerine teeth (11.8); prevomerine posterolateral shelf lacking and tooth series not sharply angled (posterolateral bony shelf present and tooth series sharply angled); dorsum lighter (darker); dark dorsolateral stripes narrower (broader); venter yellow and unpigmented (venter silvery or gray and variably pigmented).

Our analyses reveal the following characters that can also be used to differentiate *E. chamberlaini* ($n = 7$) from *E. quadridigitata* ($n = 136$; Tables 2, 4, 5): SVL 37.4–63.9% (50.4 ± 11.6) of total length (32.8–70.5% [43.6 ± 7.0]); tail width at base 4.0–7.2% (5.8 ± 1.0) of SVL (4.2–11.2% [7.7 ± 1.3]); tail laterally compressed (tail square-like in cross-section); 10 genetic autapomorphies (15 autapomorphies).

Eurycea chamberlaini ($n = 7$) can be distinguished from the western clade species ($n = 20$) by the following characters (Tables 2, 4, 5): SVL 37.4–63.9% (50.4 ± 11.6) of total length (37.6–61.6% [43.5 ± 5.2]); tail width at base 4.0–7.2% (5.8 ± 1.0) of SVL (6.7–10.1% [8.6 ± 1.0]); tail height at base 5.0–9.6% (7.6 ± 1.6) of SVL (7.9–11.9% [10.2 ± 1.3]); head width 53.4–63.3% (57.6 ± 3.3) of head length (57.9–70.9% [63.3 ± 4.0]); 10 genetic autapomorphies (48 autapomorphies).

Eurycea chamberlaini ($n = 7$) can be distinguished from the steephead/ravine clade species ($n = 20$) by the following

characters (Tables 2, 4, 5): SVL 37.4–63.9% (50.4 ± 11.6) of total length (38.1–66.1% [46.4 ± 8.3]); 15 genetic autapomorphies (5 autapomorphies).

Eurycea chamberlaini ($n = 7$) can be distinguished from the hillside seepage clade species ($n = 36$) by the following characters (Tables 2, 4, 5): SVL 37.4–63.9% (50.4 ± 11.6) of total length (37.5–51.0% [41.9 ± 3.7]); tail width at base 4.0–7.2% (5.8 ± 1.0) of SVL (5.4–10.6% [8.5 ± 1.3]); tail height at base 5.0–9.6% (7.6 ± 1.6) of SVL (8.3–11.9% [10.0 ± 1.0]); tail more laterally compressed (tail square-like in cross-section); head length 18.0–21.7% (20.2 ± 1.3) of SVL (20.0–28.7% [24.0 ± 2.0]); head depth 5.6–8.1% (6.9 ± 0.9) of SVL (7.0–12.4% [9.0 ± 1.3]); eye diameter 4.6–5.8% (5.2 ± 0.4) of SVL (4.9–8.5% [6.3 ± 0.7]); canthus length 29.8–34.0% (32.3 ± 1.5) of head length (20.7–34.5% [26.4 ± 3.4]); eye diameter 70.6–88.9% (80.6 ± 7.7) of canthus length (75–127.3% [100.6 ± 13.0]); 10 genetic autapomorphies (42 autapomorphies).

Distribution and natural history.—*Eurycea chamberlaini* is known from portions of the Piedmont in South Carolina and North Carolina, extending into the upper Coastal Plain of South Carolina and central Coastal Plain of North Carolina (Fig. 1). An apparent disjunct population in northwestern South Carolina might be contiguous with populations further south in Aiken and Barnwell Counties, South Carolina, but more-extensive sampling is required. Contrary to previous reports (Graham et al. 2008; Graham and Jensen 2011; Thawley and Graham 2012), *E. chamberlaini* is not known from Georgia or Alabama and no records of this species are known from west of the Savannah River. More extensive work is needed to determine the distribution of this species in the Carolinas and possibly in northeast Georgia. Fieldwork in the Piedmont of extreme northeastern Georgia might reveal that this species has gone undetected in that state. These efforts should be focused along small (first and second order) white-water streams and springs.

Unlike *E. quadridigitata*, this species seems to favor more-lotic environments for breeding like the five-toed species of *Eurycea*. Harrison and Guttman (2003) reported that 70% of the specimens they examined were collected near streams or seepage of spring outlets whereas 30% were associated with floodplains or ponds. However, they did not report the time of year or breeding condition of these specimens. Given the distance that *E. quadridigitata* is known to travel outside the breeding season, it might be that the animals collected near floodplains and ponds were traveling to breeding grounds or outside of the breeding season. The specimens we have collected during the breeding season were all associated with stream edges. Detailed field studies in areas of sympatry between this species and *E. quadridigitata* (e.g., Savannah River Site, in Barnwell County, South Carolina) could reveal interesting insights into the evolution of this species complex.

Remarks.—For a detailed diagnosis, description of holotype and paratypes, descriptions of larvae and adults, coloration, and etymology see Harrison and Guttman (2003).

It is unclear what the sister taxon to *E. chamberlaini* is, as results have been mixed. The work of Bonnet et al. (2014) placed their "*E. quadridigitata* 4" sample sister to their *E. chamberlaini* sample, but they did not provide specific collection data to determine what clade this specimen belonged to. Lamb and Beamer (2012) had *E. chamberlaini* sister to *E. quadridigitata* sensu stricto, the same pattern that Wray and Steppan (2016) found. However, the present study, using a gene tree–species tree approach with the most-extensive data matrix to date, found *E. chamberlaini* to be the sister taxon to the steephead/ravine clade and *E. quadridigitata* the sister clade to both. However, this relationship was not very strongly supported and the branch between the *E. quadridigitata* clade and the *E. chamberlaini* + steephead/ravine clade was very short. Further work is needed to determine the exact relationships among these three taxa; however, it is clear that they form a well-supported clade and are closely related to each other.

We caution here about attempting to identify individuals of this complex by dorsal or ventral coloration, but particularly about using ventral coloration. As Harrison and Guttman (2003) pointed out, other species may have yellow ventral coloration. In fact, we have seen yellow ventral colorations in all five species and it is the predominant coloration in all but *E. quadridigitata*. The yellow coloration seems to obscure the darker melanophore markings found elsewhere on the ventral surface, but the yellow fades rapidly in preservative, revealing this darker pigmentation. The yellow pigmentation can be observed further up the side of the body on gravid female animals (see Fig. 5A), suggesting that this coloration could be related to reproduction. This might explain the observed variability in this trait, but further work is necessary to test this hypothesis.

Eurycea quadridigitata (Holbrook 1842)
(Figs. 1, 5B–F, 6A–C, 11; Tables 2, 5)

Salamandra quadridigitata: Holbrook 1842:65. Holotype an adult female (ANSP 490 according to Fowler and Dunn [1917]) from "South Carolina, Georgia, and Florida," but restricted to "vicinity of Charleston, South Carolina" by Schmidt (1953), no collector or date reported.
Salamandra 4-digitata: Holbrook 1842:plate 21. [variant spelling].
Batrachoseps quadridigitata: Baird 1849:287.
Batrachoseps quadridigitatus: Gray 1849:42.
Manculus quadridigitatus: Cope 1869:101.
Manculus remifer: Cope 1871:84. Holotype an adult of unknown sex (lost according to Dunn 1926) from "Jacksonville, Florida," collected February 1869 by C.J. Maynard.
Manculus quadridigitata: Garman 1884:40.
Manculus quadridigitatus quadridigitatus: Stejneger and Barbour 1923:14.
Eurycea quadridigitata quadridigitata: Dunn 1923:40.
Eurycea quadridigitata remifera: Dunn 1923:40.
Manculus quadridigitatus remifer: Stejneger and Barbour 1923:14.
Eurycea quadridigitata remifer: Carr 1940:48.
Manculus quadridigitatus paludicolus: Mittleman 1947:221. [in part, misidentification]
Eurycea quadridigitata: Wake 1966:64.
Manculus quadridigitatus: Mittleman 1967:1.

Holotype.—An adult female (ANSP 490, according to Fowler and Dunn 1917) from "South Carolina, Georgia, and Florida," restricted to vicinity of Charleston, South Carolina (Schmidt 1953), no collector or date reported.

In the original description, no specimen is listed as the holotype that corresponds with the animal drawn on Plate 21 (Holbrook 1842). It was not until 75 yr later that Fowler and Dunn (1917), commenting on the salamander holdings in the Academy of Natural Sciences of Philadelphia (now the Academy of Natural Sciences of Drexel University), referenced ANSP 490 as the holotype using the name *Manculus quadridigitatus*, which is now a synonym that was first used by Cope (1869). We confirmed with Mr. Ned Gilmore, Collections Manager in the Department of Vertebrate Zoology, Academy of Natural Sciences of Drexel University that the data label on specimen ANSP 490 reads "*Manculus quadridigitatus* (Holbrook) TYPE S.C. Dr. Holbrook," indicating that this specimen was most likely tagged after 1869, 27 yr after the original description, as it is labeled with the genus *Manculus*. Mr. Gilmore also confirmed that the specimen is in poor condition, confirming the comments made by Mittleman (1967) that the specimen "is in poor condition, being soft and partially dissected."

Further complicating matters, Holbrook (1842:66) stated "This salamander is abundant in the middle section of our state [South Carolina]... Mr. Cooper and Dr. Harden have both furnished me with specimens from Georgia, and I have also received them from Florida," but gave no specific data on where the animal in Plate 21 originated from. Later authors reported the type locality as "South Carolina, Georgia, and Florida" until Schmidt (1953:56) restricted it to "the vicinity of Charleston, South Carolina." Fowler and Dunn reported the collection information of ANSP 490 as "South Carolina" which was also confirmed by Mr. Gilmore. The central portion of South Carolina is occupied by both *E. quadridigitata* and *E. chamberlaini*.

The International Commission on Zoological Nomenclature (ICZN) publishes the International Code of Zoological Nomenclature (online), which contains mandatory Articles governing zoological nomenclature. Article 75 governs the definition, designation, and usage of neotypes. Specifically, Article 75.3 lists the seven qualifications for validly designating a neotype. Given that (1) the original description of *E. quadridigitata* did not associate the plate with a specific specimen designated as the holotype; (2) 75 yr passed before a specimen claimed as the holotype was reported; (3) this specimen bears a different name and one that was not proposed until 25 yr after the original description; (4) this specimen is in very poor shape, partially dissected, and essentially destroyed; (5) at least two species originally described as *E. quadridigitata* occur in South Carolina; and (6) the present results demonstrate five species in the *E. quadridigitata* complex, three of which are morphologically similar, we designate a neotype for *E. quadridigitata* that can actually be compared morphologically and molecularly with the other four species in the complex. Our reasons listed herein, and the description that follows, meet the standards of all seven particulars (Article 75.3.1–75.3.7) for the designation of a neotype laid out in the International Commission on Zoological Nomenclature (2000).

Neotype.—An adult of unknown sex (UF178833 [KW0004], Fig. 5B) from Hanna's Hammock Rd., Tall Timbers Research Station, 1.7 mi S of CR 12, Leon County, Florida, 30.64792°N, 84.25173°W, collected 26 January 2007 by Kenneth P. Wray, E. Pierson Hill, and Joseph P. Pfaller.

Paratypes.—No paratypes listed in the original description.

Referred specimens.—FLORIDA (n = 93): one specimen (UF178902 [KW0099]) from SH 346 at River Styx, Alachua County, 29.51713°N, 82.22224°W; one specimen (UF178920 [KW0134]) from Forest Rd 235, 3.0 mi N of CR 250, Baker County, 30.37238°N, 82.39775°W; two specimens (UF178900–1 [KW0097–8]) from small pit on SE side of int SH 231 and Elijah Dobson Rd., Baker County, 30.17562°N, 82.41133°W; eight specimens (UF178839–46 [KW0010–7]) from US 301 at Santa Fe River, Bradford County, 29.83972°N, 82.16444°W; one specimen (UF24424) from 11.0 mi S and 5.5 mi W of Chipola River, Blountstown, Calhoun County, 30.2869°N, 85.1445°W; three specimens (UF68952–3, UF68955 [DBM 1442]) from btw SR 71 and CR 275, Blountstown, Calhoun County, 30.43218°N, 85.09697°W; one specimen (UF77578) from SR 20 and Chipola River, Blountstown, Calhoun County, 30.4378°N, 85.0014°W; four specimens (UF25978, UF26016, UF26031, UF26048) from Scott's Fairy, Calhoun County, 30.29547°N, 85.13158°W; two specimens (UF178931–2 [KW0145–6]) from Turkey Branch at CR 29, 1.5 mi S of US 27, Glades County, 26.90934°N, 81.32890°W; two specimens (UF129100–1 (DBM 1577]) from SR 2 and East Pittman Creek, Holmes County, 30.95007°N, 85.84155°W; one specimen (UF178838 [KW0009]) from CR 259 at Wards Creek bridge, 3.6 mi W of SR 19, Jefferson County, 30.60464°N, 83.89279°W; one specimen (UF178847 (KW0019]) from Willis Farm, SR 221, ~2 mi S of jct with SR 146 and ~0.5 mi E of SR 221, Jefferson County, 30.58279°N, 83.61742°W; three specimens (UF129117–9 [DBM 1221]) from SR 157 at Ochlockonee River, Jefferson County, 30.5854°N, 84.3592°W; four specimens (UF128860–3) from SR 59, 6.0 mi N US 100, Jefferson County, 30.27446°N, 84.04235°W; one specimen (UF129400) from 0.1 mi S of US 319 and SR 61, Apalachicola National Forest, Leon County, 30.35383°N, 84.30659°W; one specimen (UF178848 [KW0020]) from NE side of floodplain at Old Bainbridge Rd and Ochlockonee River, Leon County, 30.58623°N, 84.36208°W; two specimens (UF178904 [DBM 3413], UF178919 [KW0133]) from Ochlockonee River floodplain, Rock Bluff Botanical Area, FR 390, Leon County, 30.358056°N, 84.67861°W; six specimens (UF178831–2, UF178834–7 [KW0001, KW0003, KW0005–8]) from Hanna's Hammock Rd., Tall Timbers Research Station, 1.7 mi S of CR 12, Leon County, 30.64627°N, 84.250225°W; two specimens (UF97125–6 [DBM 2827–8]) from SR 371, Tallahassee, Leon County, 30.41348°N, 84.29692°W; eight specimens (UF77525–30, UF77532–3]) from SR 61, Tallahassee, Leon County, 30.3884°N, 84.2871°W; seven specimens (UF129197, UF129199–03, UF129210 [DBM 1209]) from US 90 at Lake Miccosukee, Leon County, 30.5289°N, 83.9809°W; 14 specimens (UF129029, UF129032, UF129034, UF 129044–6, UF129048, UF129056 [DBM 2324], UF129146–51 [DBM 2366]) from SR 12, 0.6 mi N Forest Rd 105, Apalachicola National Forest, Liberty County, 30.287°N, 85.0195°W; one specimen (UF178903 [DBM 3419]) from Apalachicola National Forest, Liberty County, 30.11694°N, 85.02388°W; one specimen (UF178930 [KW0144]) from Ochlockonee River floodplain at FH 13, 0.9 mi E of CR 67, Liberty County, 30.17731°N, 84.68351°W; three specimens

(UF129334–5, UF129337 [DBM 1987–2]) from SR 20 at Telogia Creek, Liberty County, 30.42659°N, 84.9276°W; one specimen (UF178911 [KW0125]) from near headwater of Salt Springs, Ocala National Forest, Marion County, 29.34937°N, 81.73155°W; one specimen (UF178905 [KW0117]) from near Lake Delancy, Ocala National Forest, Marion County, 29.4358°N, 81.72532°W; four specimens (UF178906–9 [KW0118–21]) from Mills Creek at US 1, Nassau County, 30.63914°N, 81.86295°W; one specimen (UF178849 [KW0023]) from SR 72, 6.5 mi E of Myakka River, Sarasota County, 27.21°N, 82.24360°W; three specimens (UF178915–7 [KW0129–31]) from small dirt road off CR 361, across from Salem Tower Rd., Tide Swamp Unit, Big Bend Wildlife Management Area, Taylor County, 29.724°N, 83.46046°W; one specimen (UF178852 [KW0026]) from Pond 4, Port Orange Wellfield, SE quadrangle USGS Daytona Quad, Volusia County, 29.07916°N, 81.13472°W; two specimens (UF178872–3 [KW0053–4]) from Choctawhatchee River drainage, 0.1 mi S of Shell Landing, Washington County, 30.53643°N, 85.85939°W.

GEORGIA (n = 28): one specimen (UF178858 [DBM 3277]) from Altamaha River swamp, Appling County, 31.92952°N, 82.27905°W; two specimens (UF129114–5 [DBM 1867]) from floodplain of Hurricane Creek, 0.25 mi S of SR 32 bridge, Bacon County, 31.535774°N, 82.444734°W; one specimen (UF178864 [KW0045]) from SH 94 at "Double Run Creek" (probably Cypress Creek, ~3–4 mi SE of Fargo), Clinch County, 30.65030°N, 82.530244°W; two specimens (UF178870–1 [KW0051–2]) from Suwannoochee Creek at SR 37, Clinch County, 31.03553°N, 82.87967°W; one specimen (UF178863 [KW0044]) from SR 119 at Run Branch, Effingham County, 32.39046°N, 81.30343°W; seven specimens (UF129062, UF129064, UF 129066, UF129069–72 [DBM 1626]) from lead water tributary of Saltilla River, 1.0 mi SSW Osierfield, Irwin County, 31.65187°N, 83.11826°W; five specimens (UF178883–7 [DBM 3276]) from blackwater creek swamp, Road 35a, DeHA 13, Fort Stewart, Long County, 31.90480°N, 81.77827°W; one specimen (UF178867 [KW0048]) from Grand Bay Wildlife Management Area, Lowndes County, 30.947331°N, 83.179975°W; two specimens (UF129102–3 [DBM 1674]) from USGS 15′ Quad, Baconton, Mitchell County, 31.38367°N, 84.16026°W; two specimens (UF128994–5 [DBM 1675]) from Sally's Branch at SR 270, Mitchell County, 31.24446°N, 84.02723°W; one specimen (UF178918 [KW0132]) from Arcadia Plantation, Thomas County, 30.76323°N, 84.01560°W; two specimens (UF178868–9 [KW0049–50]) from Cabin Branch Creek at US 84 (Greasy Branch?), Ware County, 31.10881°N, 82.56222°W; one specimen (UF178862 [KW0041]) from Little Creek at E Gardi Rd., Wayne County, 31.49093°N, 81.84744°W.

SOUTH CAROLINA (n = 14): three specimens (UF178922–4 [KW0136–8]) from Dry Bay, off of SR 1215 (Atomic Rd), 3.7 mi N of SR 64 (Dunbarton Blvd), Savannah River Site, Aiken County, 33.25007°N, 81.74614°W; three specimens (UF178925–7 [KW0139–41]) from Enchantment Bay, Savannah River Site, Barnwell County, 33.2687°N, 81.60657°W; two specimens (UF178928–9 [KW0142–3]) from Rainbow Bay, Savannah River Site, Barnwell County, 33.26313°N, 81.64329°W; one specimen (UF178910 [KW0124]) from swamp on S side of Elmwood recreation and Game Check Area off Echaw Rd., 1.3 mi N of Rutledge Rd., Francis Marion National Forest, Berkeley County, 33.21088°N, 79.47614°W; one specimen (UF178912 [KW0126]) from Wambaw Creek swamp at jct of SR 45, 0.08 mi N Honeyhill Rd., Charleston County, 33.14964°N, 79.54383°W; two specimens (UF178898–9 [KW0095–6]) from Great Pee Dee Heritage Preserve, Darlington County, 34.38628°N, 79.73387°W; one specimen (UF178921 [KW0135]) from swamp on S side of CR 119 (Sand Hills Rd), 4.2 mi W of SR 321 in Tillman, Jasper County, 32.48856°N, 81.17045°W; one specimen (UF178897 [KW0094]) from Woods Bay State Natural Area, Sumter County, 33.94761°N, 79.97958°W.

Diagnosis.—A small species of *Eurycea* that can be distinguished from all other US plethodontids by the presence of four toes on the hindlimb (five in other species), except *Hemidactylium scutatum* and the four other species discussed herein. This species is distinguished from *H. scutatum* by the absence of a basal tail constriction (present in *H. scutatum*) and a silvery or light-gray venter with diffused flecking of darker pigments near edges (white with prominent black spots). *Eurycea quadridigitata* can be distinguished from the other members of the complex by the characters listed in the following comparisons section.

Comparisons.—Characters separating *E. quadridigitata* from each of the other members of the species complex are listed herein, followed by character states of other species in parentheses.

The following characters were used to distinguish *Eurycea quadridigitata* from *E. chamberlaini* in the original description of the latter (Harrison and Guttman 2003): limbs relatively shorter (relatively longer); 17–18 costal grooves (15–16); average of 11.8 prevomerine teeth (10); prevomerine posterolateral bony shelf present and tooth series sharply angled (posterolateral shelf lacking and tooth series not sharply angled); dorsum darker (lighter); dark dorsolateral stripes broader (narrower); venter silvery or gray and variably pigmented (yellow and unpigmented).

Our analyses reveal the following characters that can be used to differentiate *Eurycea quadridigitata* (n = 136) from *E. chamberlaini* (n = 7; Tables 2, 4, 5): SVL 32.8–70.5% (43.6 ± 7.0) of total length (37.4–63.9% [50.4 ± 11.6]); tail width at base 4.2–11.2% (7.7 ± 1.3) of SVL (4.0–7.2% [5.8 ± 1.0]); tail square-like in cross-section (tail more laterally compressed); 15 genetic autapomorphies (10 autapomorphies).

Eurycea quadridigitata (n = 136) can be distinguished from the western clade species (n = 20) by the following characters (Tables 2, 4, 5): 20.8–33.8 mm (26.7 ± 2.4) SVL (22.3–37.2 mm [30.5 ± 4.0]); tail width at base 4.2–11.2% (7.7 ± 1.3) of SVL (6.7–10.1% [8.6 ± 1.0]); tail height at base 6.3–13.4% (9.2 ± 1.3) of SVL (7.9–11.9% [10.2 ± 1.3]); head depth 5.5–10.5% (7.1 ± 0.8) of SVL (6.1–9.9% [7.8 ± 0.8]); interocular distance 3.9–7.4% (5.5 ± 0.6) of SVL (5.0–8.0% [6.0 ± 0.7]); canthus length 23.2–40.5% (30.7 ± 3.2) of head length (27.3–36.1% [32.9 ± 2.6]); 15 genetic autapomorphies (48 autapomorphies).

Eurycea quadridigitata (n = 136) can be distinguished from the steephead/ravine clade species (n = 20) by the following characters (Tables 2, 4, 5): 20.8–33.8 mm (26.7 ± 2.4) SVL (18.0–29.5 mm [23.8 ± 3.5]); head length 15.4–

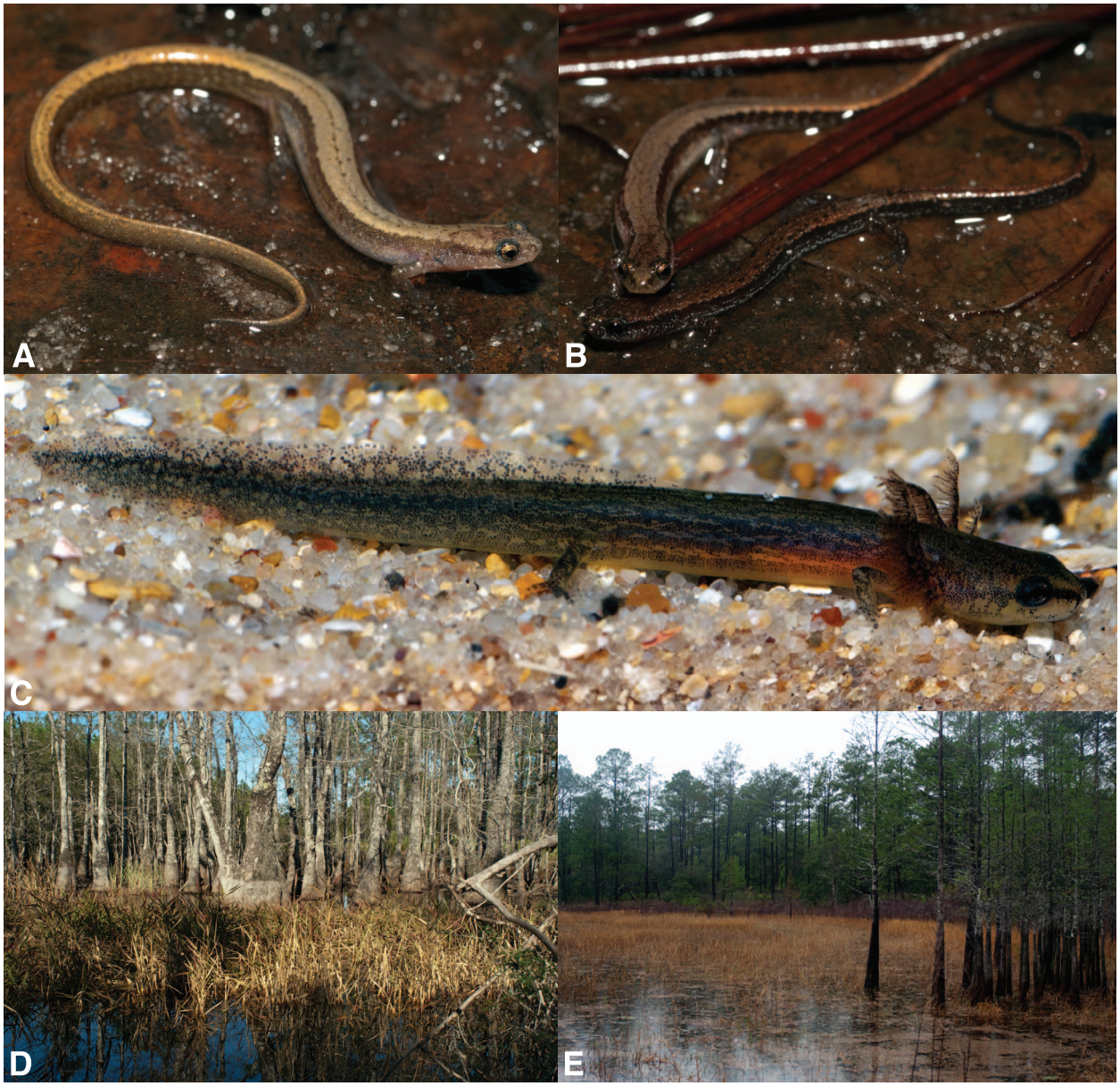

FIG. 6.—*Eurycea quadridigitata* complex. (A) *E. quadridigitata* (KW0126): adult female from Berkeley County, South Carolina; (B) *E. quadridigitata*: gravid female (top) and adult male from Wakulla County, Florida. (C) *E. quadridigitata*: larva from Liberty County, Florida; (D) *E. quadridigitata* breeding habitat: cypress dome, Liberty County, Florida; (E) *E. quadridigitata* breeding habitat: sandhill pond edged with *Taxodium* sp.

24.4% (19.9 ± 1.6) of SVL (18.9–24.4% [21.5 ± 1.8]); head width 8.1–14.2% (12.0 ± 0.8) of SVL (11.0–14.4% [12.9 ± 1.0]); head depth 5.5–10.5% (7.1 ± 0.8) of SVL (6.3–9.4% [8.0 ± 0.7]); interocular distance 3.9–7.4% (5.5 ± 0.6) of SVL (5.1–9.4% [6.5 ± 1.0]); 15 genetic autapomorphies (5 autapomorphies).

Eurycea quadridigitata (n = 136) can be distinguished from the hillside seepage clade species (n = 36) by the following characters (Fig. 11; Tables 2, 4, 5): tail width at base 4.2–11.2% (7.7 ± 1.3) of SVL (5.4–10.6% [8.5 ± 1.0]); tail height at base 6.3–13.4% (9.2 ± 1.3) of SVL (8.3–11.9% [10.0 ± 1.0]); hindlimb length 21.7–31.9% (26.7 ± 2.3) of SVL (24.6–35.0% [28.4 ± 2.1]); forelimb length 17.0–26.7% (22.3 ± 2.2) of SVL (19.6–29.1% [24.1 ± 2.3]); head length 15.4–24.4% (19.9 ± 1.6) of SVL (20.0–28.7% [24.0 ± 2.0]); head width 8.1–14.2% (12.0 ± 0.8) of SVL (11.5–15.5% [13.3 ± 1.0]); head depth 5.5–10.5% (7.1 ± 0.8) of SVL (7.0–12.4% [9.0 ± 1.3]); interocular distance 3.9–7.4% (5.5 ± 0.6) of SVL (5.0–9.8% [6.8 ± 1.1]); eye diameter 4.1–6.7% (5.3 ± 0.5) of SVL (4.9–8.5% [6.3 ± 0.7]); head width 45.5–77.5% (60.6 ± 5.5) of head length (41.8–64.7% [55.5 ± 3.9]); canthus length 23.2–40.5% (30.7 ± 3.2) of head length (20.7–34.5% [26.4 ± 3.4]); interocular distance 32.4–61.9% (46.5 ± 5.2) of width (41.4–64.0% [51.4 ± 5.7]); ocular diameter 64.7–127.3% (88.1 ± 10.0) of canthus length (75.0–127.3% [100.6 ± 13.0]); 15 genetic autapomorphies (42 autapomorphies).

Description of neotype.—SVL = 27.3 mm; TL = 35 mm; TW = 1.9 mm; TH = 2.2 mm; HLL = 7.1 mm; FLL = 6.0 mm; HL = 5.1 mm; HW = 3.1 mm; HD = 1.8 mm; CL = 1.5 mm; IO = 1.5 mm; OD = 1.4 mm.

Head rounded in dorsal view and slightly protruding in lateral view. The head length is 18.7% of the SVL and 11.4% of SVL at the widest point. The head width at the widest point is 60.8% of head length. Head depth is 6.6% of SVL. Interocular distance is 48.4% of the head at widest point. Snout length is 29.4% of head length and eye diameter is 93.3% of snout length. The SVL is 43.8% of total length. The tail is complete and is 56.2% of the total length. The tail base is square in cross-section, but wedge-shaped at distal end. A keel is present on the dorsum of the tail. The forelimbs are 22.0% of the SVL with four digits present on each manus and the hindlimbs are 26.0% of the SVL with four digits on each pes.

In life (Fig. 5B) the dorsum is bronzish, almost forming a broad stripe, with sparse, irregular, dark brown spots. A dark brown dorsolateral stripe originating behind each eye extends laterally onto the body and ends toward the tail tip. A series of dark brown broken lines are present in the dark field on the side of the body. Bluish-white flecking is concentrated from the tip of the snout to below the dorsolateral line on the side of the head. These flecks are largely absent from the sides of the body but become conspicuous again near the hindlimbs and proximal end of tail. Venter is silvery-gray in color with dark melanophores concentrated near the underside of the head, gular region, sides of the venter, and near the cloaca and underside of tail. The iris of the eye is golden with a dark lateral stripe bisecting the pupil horizontally.

In preservation, the dorsum is darker brown, but irregular spots are still present. The sides are darker and the flecking is faded to a cream white color and less apparent than in life. The venter is a dull grayish coloration, but melanophores are still present. The eye is opaque.

Description.—The following description is based off of 136 measured individuals. Variation in the 17 ratios for the 136 animals examined is listed in Table 2 (for variation in the 13 morphometric characters see Supplemental Table S2). Molecular variation for six loci is listed in Table 5.

The snout is rounded in dorsal view, slightly protruding in lateral view, and is 23.2–40.5% (30.7 ± 3.2) of head length. The nares are small and cirri are present in males during breeding season. The eyes are protuberant, but barely visible when viewed from underneath. Eye diameter is 64.7–127.3% (88.1 ± 10.0) of the snout length and the distance between the eyes is 32.4–61.9% (46.5 ± 5.2) of the widest part of head. The head is block-shaped, with the width 45.5–77.5% (60.6 ± 5.5) of the length head. The head length is 15.4–24.4% (19.9 ± 1.6%) of the SVL length.

Total length ranges from 33.9–90.5 mm (62.6 ± 10.2) while SVL averages 20.8–33.8 mm (26.7 ± 2.4). The SVL is 32.8–70.5% (43.6 ± 7.0) of the total length. Costal grooves ranged from 14–17. The forelimbs and hindlimbs are 17.0–26.7% (22.3 ± 2.2) and 21.7–31.9% (26.7 ± 2.3) of the SVL, respectively. The forelimb-to-hindlimb ratio ranges from 67.2–98.6% (83.6 ± 7.0). The manus and pes have four digits each.

Tail length is 29.5–67.2% (56.4 ± 7.0) of total length. The width and height of the basal portion of the tail is 4.2–11.2% (7.7 ± 1.3) and 6.3–13.4% (9.2 ± 1.3), respectively. In cross-section, the tail is square-like, becoming wedge-shaped distally with an obvious keel present in most specimens.

Color is highly variable in this species and animals can undergo metachrosis seemingly triggered, in part, due to temperature, stress, and/or activity levels (Figs. 5B–F, 6A–B). Dorsal coloration can be dark brown, tan, bronze, coppery-orange, or yellow. The dorsum may be marked with flecking or larger, irregular spots of darker pigment. Often a thin, dark stripe is present on the midline that may become broken into a dashed line. A herring bone pattern of darker pigment is also common in some individuals. The dark brown or blackish dorsolateral stripe begins behind the eye and extends onto the side of the body and tail. It is often present through the eye to the tip of the snout as a series of lighter smudge marks. When an animal undergoes a chromatic change to a light phase, the stripe is usually thinner and well defined, but during the dark phase, the stripe becomes thicker and often encompasses the entire side of the animal. Whitish to bluish flecking is common around the sides of the head and body but can be quite variable and is affected by chromatic changes.

The venter is most often a silvery or off-white coloration but can be a dark gray. However, occasional individuals may have yellow on the venter, though it is most often limited to the underside of the tail and hindlimb region. Darker melanophores are common near the edges of the venter and around the underside of the head and tail. Individuals with yellow on the venter usually do not have melanophores present in the yellow coloration. Often a bright, silvery streak is located along the midline of the ventral surface. This is the result of the peritoneal lining showing through the thin skin of the ventral surface.

Larva.—The larvae of this species have a dark ground color that ranges from almost black to dark gray (Fig. 6C). The dorsum, sides, and limbs are covered with small, yellowish vermiculations that turn into spots on the tail. A dark line runs along the canthus rostralis, through the eye, but fades on the rear of the head. The ventral tail fin inserts at the midpoint of the tail. The dorsal tail fin inserts far onto the dorsum of the body at a point anterior to the hindlimb insertions, similar to the larvae of *E. chamberlaini*.

Etymology.—The specific epithet is derived from Latin *quadra*: four; Latin *digita*: a finger or toe; Latin *ata*: having; *quadridigitata*: an adjective in the nominative singular formed to mean "having four toes"; in reference to the four toes found on the hind feet in contrast to the ancestral five-toed condition found in most other salamanders. We recommend the common name of Southeastern Dwarf Salamanders for this species.

Distribution and natural history.—*Eurycea quadridigitata* is known throughout the Coastal Plain from southern North Carolina southward through the eastern half of South Carolina and into southern Georgia and all of Florida. To the west, we have only been able to verify it in extreme southwestern Alabama and extreme eastern Louisiana (Fig. 1). It is likely this species occurs in the coastal cypress wetlands of southern Alabama and Mississippi, but targeted collections are needed. *Eurycea quadridigitata* has been documented to occur in a handful of sites with *E. chamberlaini* in Barnwell County, South Carolina (Harrison and Guttman 2003). It also occurs in close proximity with the undescribed steephead/ravine and hillside seepage species in the central panhandle of Florida and the western clade in eastern Louisiana.

FIG. 7.—*Eurycea quadridigitata* complex. (A) *E. paludicola*: adult from Tyler County, Texas; (B) *E. paludicola* (KW0981): adult from Houston County, Texas; (C) *E. paludicola* (KW1021): adult from Ouachita County, Arkansas; (D) *E. paludicola*: adult from Nevada County, Arkansas (Photo courtsey of Kory G. Roberts).

Much of what has been published to date on *Eurycea quadridigitata* sensu lato most likely applies to this species (see Petranka 1998 for thorough review). Although this species can be found in a variety of terrestrial and aquatic habitats, we have observed that this species utilizes breeding wetlands associated with cypress (*Taxodium* spp.; Fig. 6D–E). Future work focusing on this relationship should provide unique insights on the natural history and evolutionary biology of this species. See remarks section for *E. chamberlaini* for discussion on the taxonomic position of this species.

Eurycea paludicola comb. nov. (Mittleman 1947)
(Figs. 1, 7A–D; Tables 2, 5)

Manculus quadridigitatus paludicolus: Mittleman 1947:220. Holotype an adult male (USNM 123979) from "Louisiana, Grant Parish, Pollock," collected 6–9 September 1937 by Percy Viosca, Jr.

Manculus quadridigitatus uvidus: Mittleman 1947:221. Holotype an adult male (USNM 123980; formerly BU 2338) from "Gayle, Caddo Parish, Louisiana," collected on unknown date by John K. Strecker and Lorraine S. Frierson, Jr. [**new synonymy**]

Manculus quadridigitatus: Mittleman 1967:1. [in part, misidentification]

Holotype.—An adult male (USNM 123979) from Pollock, Grant Parish, Louisiana, 31.5253°N, 92.4071°W, collected 6–9 September 1937 by Percy Viosca, Jr.

Paratypes.—LOUISIANA (n = 75): five specimens (UMMZ 75940), Bienville, Bienville Parish; one specimen (Percy Viosca private collection [= PV]), Indian Mound, East Baton Rouge Parish; eight specimens (UMMZ 75941) from Evangeline Parish, no other data; eight specimens (PV) from Pollock, Grant Parish; one specimen (PV) from 5 mi W of Jonesboro, Jackson Parish; two specimens (PV) from Harahan, Jefferson Parish; six specimens (PV) from Bohon, Jefferson Parish; five specimens (PV) from 8 mi S of Marreto, Jefferson Parish; five specimens (PV) from Fishville, La Salle Parish; four specimens (PV) from Kisatchie, Natchitoches Parish; two specimens (PV) from Monroe, Ouachita Parish; nine specimens (PV) from 10 mi W of Alexandria, Rapides Parish; one specimen (PV) from Forest Hill, Rapides Parish; two specimens (USNM 99176–7) from 4 mi SW of Many, Sabine Parish; one specimen (CAS 11292) from 2 mi NW of Many, Sabine Parish; one specimen (PV) from Greensburg, St. Helena Parish; one specimen (PV) from Mandeville, St. Tammany Parish; ten specimens (PV) from Covington, St. Tammany Parish; two specimens (PV) from Pearl River, St. Tammany Parish; one specimen (PV) from Sheridan, Washington Parish.

TEXAS (n = 28): one specimen (USNM 17700) from Palestine, Anderson County; five specimens (Bryce C. Brown private collection [= BCB] BCB 485, BCB 753–6) from 6 mi E of Kenney, Austin County; two specimens (Floyd E. Potter Jr. private collection [= FP] FP28, FP30) from 2 mi E of Industry, Austin County; 14 specimens (BCB 1327–8, BCB 1568–71, M. B. Mittleman private collection,

TCWC 1198–1204) from Normangee State Park, near Normangee, Leon County; four specimens (USNM 99773–6) from 5 mi SW of Pendleton Ferry, Sabine County; one specimen (USNM 99762) from Hillister, Tyler County.

Referred specimens.—LOUISIANA ($n = 10$): one specimen (UF178853 [DBM 3246]) from deeply gullied ravines, Sicily Island Hills Wildlife Management Area, Catahoula Parish, 31.82444°N, 91.75166°W; nine specimens (UF128913–21 [DBM 1688]) from lower Mississippi River delta, end of Lakewood Drive, 0.7 mi S of US 90, Luling, St. Charles Parish 29.90515°N, 90.34927°W.

TEXAS ($n = 10$): six specimens (UF129104–9 [DBM 1025]) from 5.0 mi N of Atlanta, 0.25 mi W of US 59, Cass County, 33.18675°N, 94.15530°W; four specimens (UF178854–7 [TJH 1510–3]) from Pond 17-1, Angelina National Forest, San Augustine County, 31.33419°N, 94.22290°W.

Diagnosis.—A moderate-sized species of *Eurycea* distinguished from all other US plethodontids, except *H. scutatum* and the four other species discussed herein, by the presence of four toes on the pes (five in other species). *Eurycea paludicola* can be separated from *H. scutatum* by the absence of a basal tail constriction (present in the latter) and a ventral surface that is silver, gray, or yellow and lacks large black spots (white with black spots in *H. scutatum*). *Eurycea paludicola* can be distinguished from the other members of the complex by the characters listed in the following comparisons section.

Comparisons.—Characters separating *E. paludicola* from each of the other members of the species complex are listed herein, followed by character states of other species in parentheses.

The following characters can be used to distinguish *E. paludicola* ($n = 20$) from *E. chamberlaini* ($n = 7$; Tables 2, 4, 5): SVL 37.6–61.6% (43.5 ± 5.2) of total length (37.4–63.9% [50.4 ± 11.6]); tail width at base 6.7–10.1% (8.6 ± 1.0) of SVL (4.0–7.2% [5.8 ± 1.0]); tail height at base 7.9–11.9% (10.2 ± 1.3) of SVL (5.0–9.6% [7.6 ± 1.6]); head width 53.4–63.3% (57.6 ± 3.3) of head length (57.9–70.9% [63.3 ± 4.0]); 48 genetic autapomorphies (10 autapomorphies).

Eurycea paludicola ($n = 20$) can be distinguished from *E. quadridigitata* ($n = 136$) by the following characters (Tables 2, 4, 5): 22.3–37.2 mm (30.5 ± 4.0) SVL (20.8–33.8 mm [26.7 ± 2.4]); tail width at base 6.7–10.1% (8.6 ± 1.0) of SVL (4.2–11.2% [7.7 ± 1.3]); tail height at base 7.9–11.9% (10.2 ± 1.3) of SVL (6.3–13.4% [9.2 ± 1.3]); head depth 6.1–9.9% (7.8 ± 0.8) of SVL (5.5–10.5% [7.1 ± 0.8]); interocular distance 5.0–8.0% (6.0 ± 0.7) of SVL (3.9–7.4% [5.5 ± 0.6]); canthus length 27.3–36.1% (32.9 ± 2.6) of head length (23.2–40.5% [30.7 ± 3.2]); 48 genetic autapomorphies (15 autapomorphies).

Eurycea paludicola ($n = 20$) can be distinguished from the steephead/ravine clade species ($n = 20$) by the following characters (Tables 2, 4, 5): 22.3–37.2 mm (30.5 ± 4.0) SVL (18.0–29.5 mm [23.8 ± 3.5]); tail width at base 6.7–10.1% (8.6 ± 1.0) of SVL (5.0–9.4% [7.0 ± 1.2]); tail height at base 7.9–11.9% (10.2 ± 1.3) of SVL (7.8–10.5% [9.1 ± 0.8]); forelimbs 18.5–23.8% (21.3 ± 1.5) of SVL (20.7–26.8% [23.6 ± 1.5]); canthus length 27.3–36.1% (32.9 ± 2.6) of head length (22.6–34.0% [29.1 ± 3.1]); 48 genetic autapomorphies (5 autapomorphies).

Eurycea paludicola ($n = 20$) can be distinguished from the hillside seepage clade species ($n = 36$) by the following characters (Tables 2, 4, 5): 22.3–37.2 mm (30.5 ± 4.0) SVL (16.4–25.7 mm [22.7 ± 2.2]); forelimbs 18.5–23.8% (21.3 ± 1.5) of SVL (19.6–29.1% [24.1 ± 2.3]); hindlimbs 21.2–31.4% (26.0 ± 3.0) of SVL (24.6–35.0% [28.4 ± 2.1]); head length 17.3–24.7% (19.9 ± 1.8) of SVL (20.0–28.7% [24.0 ± 2.0]); eye diameter 4.3–7.2% (5.7 ± 0.7) of SVL (4.9–8.5% [6.3 ± 0.7]); head width 57.9–70.9% (63.3 ± 4.0) of head length (41.8–64.7% [55.5 ± 3.9]); canthus length 27.3–36.1% (32.9 ± 2.6) of head length (20.7–34.5% [26.4 ± 3.4]); eye diameter 70.0–100.0% (87.5 ± 10.2) of canthus length (75.0–127.3% [100.6 ± 13.0]); 48 genetic autapomorphies (42 autapomorphies).

Description of holotype.—See Mittleman (1947) for description of holotype.

Description.—The following description is based off of 20 measured individuals. Variation in the 17 ratios for the 20 animals examined is listed in Table 2 (for variation in the 13 morphometric characters see Supplemental Table S2). Molecular variation for six loci is listed in Table 5.

Snout is rounded in dorsal view and slightly protruding-to-rounded in lateral view. The snout ranges from 27.3–36.1% (32.9 ± 2.6) of the head length. The nares are small and cirri are present in males during breeding season. The eyes are protuberant but barely visible when viewed ventrally. The eye diameter ranges 70.0–100.0% (87.5 ± 10.2) of the canthus length and the interocular distance is 41.2–57.9% (48.0 ± 4.0) of the head width. The head width ranges from 57.9–70.9% (63.3 ± 4.0) of the head length, which is 17.3–24.7% (19.9 ± 1.8) of the SVL.

Total length is 45.8–87.4 mm (71.1 ± 13.4) and the SVL is 22.3–37.2 mm (30.5 ± 4.0). Costal groove ranges from 14–17. The forelimbs and hindlimbs range from 18.5–23.8% (21.3 ± 1.5) and 21.2–31.4% (21.3 ± 1.5) of the SVL, respectively. The forelimb-to-hindlimb ratio ranges from 72.4–100.0% (83.0 ± 9.2). The manus and pes have four digits each.

Tail length is 38.4–62.4% (56.5 ± 5.2) of the total length. The width and height of the basal portion of the tail is 6.7–10.1% (8.6 ± 1.0) and 7.9–11.9% (10.2 ± 1.3), respectively. In cross-section, the tail base is square, becoming laterally compressed toward the distal end. An obvious tail keel is present on most specimens.

As with other species in this complex, coloration is highly variable in *E. paludicola* (Fig. 7A–D) and individuals are capable of undergoing metachrosis. Dorsal coloration can be dark brown, bronze, tan, or yellow, usually with a lighter, broad dorsal stripe that extends onto the tail. This stripe is just as variable, variably being some shade of brown, coppery-orange, or yellow, and is often brighter on the posterior portion of the body and tail. As with other members of the complex, the dorsal stripe is variably spotted with flecking or irregular spots, may be distinctive or broken, or appear as a herring bone pattern running the length of the body. The dorsum of the head is usually marked with irregular spotting. The dorsolateral stripe may be indistinctly marked on the canthus rostralis, but is usually prominent starting behind the eye and extending onto the body through to the tip of the tail, though it is often less distinct on the tail. The width of the dorsolateral stripe varies, but it is usually thinner and more-distinctly set off from the background

coloration than in *E. quadridigitata*. White, grayish, and/or bluish flecking is usually present on the head below the canthus and postorbital stripe and on the body and proximal portions of the tail below the dorsolateral stripe. This flecking is occasionally seen on the dorsum of the head and body, but it is rare and diffuse when present. The sides of the body below the dorsolateral stripe may be dark brown to light gray but are always in stark contrast to the ground color of the dorsum. Other than the aforementioned flecking, the sides of the body are relatively free of markings. The dorsum of the hindlimbs and forelimbs are usually colored the same as the sides, though the dorsum of the hindlimbs occasionally has the coloration of the dorsum of the body.

The ventral coloration may be dark gray, off-white, or yellow. The former colors are prominent in some areas, but animals with yellow venters can be found throughout the range of this species and in some areas it is the dominant coloration. As in *E. quadridigitata*, the yellow coloration is most-often confined to the tail and groin region; however, specimens with entirely yellow ventral regions (including the head and gular region) are not uncommon, particularly in the northern portion of the range (Fig. 7D). Grayish melanophores may be present throughout the ventral region or absent entirely, regardless of the coloration. It is unclear whether this is due to metachrosis or a fixed pattern. Unlike in *E. quadridigitata*, a silvery midventral stripe is usually not evident.

Larva.—We have not examined any larvae of this species and are unaware of any detailed description of larvae that can be attributed to this species.

Etymology.—The specific epithet is derived from the Latin *palude*: bog, fen, marsh, swamp; Latin suffix *-cola*: inhabitant, dweller; *paludicola*: adjective in the nominative singular formed to mean "inhabitant of swamps or marshes"; presumably in reference to the typical habitats in which this species can be found. We recommend the common name of Western Dwarf Salamanders for this species.

Distribution and natural history.—This species is known from throughout the eastern third of Texas, eastward into portions of southern Arkansas, most of Louisiana, and eastern Mississippi. It is unclear how far east this species ranges, but we have verified a record from as far east as Jones County, Mississippi, within 30 mi of the Alabama border (Fig. 1). This species is known to occur within close proximity of *E. quadridigitata* in St. Tammany Parish, Louisiana and probably occurs with it in parts of southern Mississippi. The Jones County, Mississippi record is further east than the most-western record of the undescribed hillside seepage species, making it possible that these two species occur in close proximity. Further sampling during the breeding season in eastern Louisiana, southern Mississippi, and western Alabama, paying close attention to habitat, is necessary to understand the full extent of this species range.

Most of the natural history work on *E. quadridigitata* sensu lato applies to the species further east, particularly *E. quadridigitata* sensu stricto. Despite being common in many areas of Texas and Louisiana, much is still unknown about the biology of this species. Future work is needed to fully understand the natural history of this species.

Remarks.—Several studies have shown that this species is more-closely related to the neotenic *Eurycea* of the Edwards Plateau in central Texas than to the other four species in the complex (Bonett et al. 2014; Lamb and Beamer 2012; Wray and Steppan 2016). The specific epithet *paludicolus* was first applied to animals from southern Louisiana and eastern Texas as *Manculus quadridigitatus paludicolus* (Mittleman 1947). However, 20 yr later, this subspecies was no longer recognized and any variation originally described was considered to be clinal in nature (Mittleman 1967). Consequently, care should be taken to ascertain which biological and natural history information from previous studies of *E. quadridigitata* sensu lato applies to *E. paludicola*. Additionally, at least two deep genetic lineages exist within this species, warranting future investigation (Fig 2).

Mittleman (1947) originally described *M. q. paludicolus* and *M. q. uvidus* (in this order) before later considering both subspecies to be invalid and placing them into the synonymy of *M. quadridigitatus* (Mittleman 1967). The animals once described as *M. q. uvidus* now fall under the description of *E. paludicola*, making this name a junior synonym of *E. paludicola*.

Eurycea ***hillisi*** sp. nov.
(Figs. 1, 8A–F; Tables 2, 5)

Manculus quadridigitatus quadridigitatus: Mittleman 1947:219. [in part, misidentification]
Manculus quadridigitatus: Mittleman 1967:1. [in part, misidentification]

Holotype.—An adult of unknown sex (UF178829 [DBM 4066], Fig. 8A–C) from under small sphagnum mat on slope above floodplain amidst thin layer of hardwood leaf litter on sandy soil, northwest side of intersection of Chipola River and State Road 20, Calhoun County, Florida, 30.433486°N, 85.171278°W, collected 11 October 2016 by D. Bruce Means.

Paratypes.—ALABAMA ($n = 3$): one specimen (UF178875 [DBM 3187A]) from USGS Tuskegee Quad, Tuskegee National Forest, Macon County, 32.43136°N, 85.64634°W; two specimens (UF178860, UF178888 [DBM 3186]) from USGS Loachapoka Quad, Macon County, 32.51466°N, 85.60421°W.

FLORIDA ($n = 3$): one specimen (UF178865 [TDH 1658]) from under log, ~50 yd NNW of boat ramp, Chipola River at SR 20, Calhoun County, 30.431944°N, 85.17166°W; one specimen (UF178830 [DBM 4066], Fig. 8D–F) from northwest side of intersection of Chipola River and State Road 20, Calhoun County, 30.433486°N, 85.171278°W; one specimen (UF178882 [DBM 3272]) from Rich Pouncy Bog, Rich Pouncy Property, Washington County, 30.45472°N, 85.50944°W; one specimen (UF178861 [DBM 3279]) from small creek draining Falling Waters Hill, just NW of large impoundment and upsite of falls, Washington County, 30.72793°N, 85.53270°W.

Referred specimens.—ALABAMA ($n = 8$): one specimen (UF178859 [DBM 3187B]) from USGS Little Texas Quad, Tuskegee National Forest, Macon County, 32.48679°N, 85.60377°W; four specimens (UF178874, UF178876–8 [DBM 3187A]) from USGS Tuskegee Quad, Macon County, Tuskegee National Forest, 32.43136°N, 85.64634°W; three specimens (UF178889–91 [DBM 3186])

FIG. 8.—*Eurycea quadridigitata* complex. (A) *E. hillisi* (UF178829): holotype from Calhoun County, Florida; (B) *E. hillisi* (UF178829): holotype from Calhoun County, Florida; (C) *E. hillisi* (UF178829): ventral aspect of holotype from Calhoun County, Florida; (D) *E. hillisi* (UF178830): paratype from Calhoun County, Florida; (E) *E. hillisi* (UF178830): paratype from Calhoun County, Florida; (F) *E. hillisi* (UF178830): ventral aspect of paratype from Calhoun County, Florida.

from USGS Loachapoka Quad, Macon County, 32.51466°N, 85.60421°W.

FLORIDA (n = 3): three specimens (UF178879–81 [DBM 3272]) Rich Pouncy Bog, Rich Pouncy Property, Washington County, 30.45472°N, 85.50944°W.

GEORGIA (n = 4): one specimen (GMNH 49991 [SPG0014]) from US 341, 50 m S of town of Roberta, Crawford County, 32.69609°N, 84.00915°W; one specimen (GMNH 49989 [SPG0004]) from Mt. Sinai Road, ~3 mi NE of Gay, Joe Kurz Wildlife Management Area, Meriwether County, 33.11985°N, 84.52662°W; one specimen (UF178866 [KW0047]) from ~1 mi N of Junction City, Talbot County, 32.61975°N, 84.43719°W; one specimen (GMNH 49990 [SPG0013]) from SR 208, 10 mi E of Talbotton, Taylor County, 32.64611°N, 84.37728°W.

Diagnosis.—A small *Eurycea* that is distinguishable from all other US plethodontids by the presence of four toes on the hindlimb (five in all others) except for *H. scutatum*, from which it can be distinguished by the absence of a basal tail constriction and lack of a white venter with large black spots, and from other members of this species complex. *Eurycea hillisi* is distinguishable from other members of this complex by the characters listed in the following comparisons section.

Comparisons.—Characters separating *E. hillisi* from each of the other members of the species complex are listed herein, followed by character states of other species in parentheses.

The following characters can be used to separate *E. hillisi* ($n = 20$) from *E. chamberlaini* ($n = 7$; Tables 2, 4, 5): SVL 38.1–66.1% (46.4 ± 8.3) of total length (37.4–63.9% [50.4 ± 11.6]); 5 genetic autapomorphies (10 autapomorphies).

Eurycea hillisi ($n = 20$) can be distinguished from *E. quadridigitata* ($n = 136$) using the following (Tables 2, 4, 5): 18.0–29.5 mm (23.8 ± 3.5) SVL (20.8–33.8 mm [26.7 ± 2.4]; head length 18.9–24.4% (21.5 ± 1.8) of SVL (15.4–24.4% [19.9 ± 1.6]); head width 11.0–14.4% (12.9 ± 1.0) of SVL (8.1–14.2% [12.0 ± 0.8]); head depth 6.3–9.4% (8.0 ± 0.7) of SVL (5.5–10.5% [7.1 ± 0.8]); interocular distance 5.1–9.4% (6.5 ± 1.0) of SVL (3.9–7.4% [5.5 ± 0.6]); 5 genetic autapomorphies (15 autapomorphies).

Eurycea hillisi ($n = 20$) can be distinguished from *E. paludicola* ($n = 20$) with the following characters (Tables 2, 4, 5): 18.0–29.5 mm (23.8 ± 3.5) SVL (22.3–37.2 mm [30.5 ± 4.0]); tail width at base 5.0–9.4% (7.0 ± 1.2) of SVL (6.7–10.1% [8.6 ± 1.0]); tail height at base 7.8–10.5% (9.1 ± 0.8) of SVL (7.9–11.9% [10.2 ± 1.3]); forelimbs 20.7–26.8% (23.6 ± 1.5) of SVL (18.5–23.8% [21.3 ± 1.5]); canthus length 22.6–34.0% (29.1 ± 3.1) of head length (27.3–36.1% [32.9 ± 2.6]); 5 genetic autapomorphies (48 autapomorphies).

Eurycea hillisi ($n = 20$) is distinguishable from the hillside seepage clade species ($n = 36$) using the following traits (Tables 2, 4, 5): tail width at base 5.0–9.4% (7.0 ± 1.2) of SVL (5.4–10.6% [8.5 ± 1.3]); tail height at base 7.8–10.5% (9.1 ± 0.8) of SVL (8.3–11.9% [10.0 ± 1.0]); head length 18.9–24.4% (21.5 ± 1.8) of SVL (20.0–28.7% [24.0 ± 2.0]); eye diameter 5.1–6.7% (5.7 ± 0.5) of SVL (4.9–8.5% [6.3 ± 0.7]); head width 56.7–66.0% (60.3 ± 2.7) of head length (41.8–64.7% [55.5 ± 3.9]); 5 genetic autapomorphies (42 autapomorphies).

Description of holotype.—SVL = 23.4 mm; TL = 34.0 mm; TW = 2.2 mm; TH = 2.3 mm; HLL = 6.6 mm; FLL = 6.0 mm; HL = 5.3 mm; HW = 3.1 mm; HD = 2.2 mm; CL = 1.2 mm; IO = 2.2 mm; OD = 1.3 mm.

The head is rounded in dorsal view and rounded, but slightly protruding, in lateral view. The head length is 22.6% of the SVL and the head is 13.2% of the SVL at the widest point. The head width is 58.5% of head length at the widest point and the head depth is 9.4% of the SVL. Interocular distance is 71.0% of the head at the widest point. The snout is 22.6% of the head length and the eye diameter is 108.3% of snout length. The SVL is 40.8% of the total length. The tail is complete and 59.2% of the total length. The base of the tail is round in cross-section throughout the length. The forelimbs are 25.6% of the SVL with four digits on each manus and the hindlimbs are 28.2% of the SVL with four digits on each pes.

In life (Fig. 8A–B), the dorsum of head and anterior of body are coppery-brown, fading to a coppery-orange on posterior and tail. A faint, grayish, herring bone pattern is present, beginning just posterior to the insertion of forelimbs and extending to just past the insertion of the hindlimbs where it abruptly ends. The dorsolateral stripe begins faintly at the nares, extends through the eye, and continues to tip of the tail. The dorsolateral stripe is faintest on the head and anterior portion of the body, becoming slightly broader and darker on the posterior portion of the body, and darkest on the anterior portion of the tail where it also becomes broadest, before becoming lighter towards the tip of the tail. Gray to white flecks are evident on the head, most commonly below the canthus rostralis and the dorsolateral stripe, but they are also scattered dorsally in the interorbital region and snout. These flecks occur along the flanks of the body, particularly below the dark dorsolateral line but also dorsally along this line. Very few of these flecks are evident on the tail. The forelimbs are colored similarly to the dorsum. The hindlimbs are similar but have a bright coppery-orange patch restricted to the proximal dorsal surface of the limbs. Dark pigment surrounds both eye lids and nares. The eyes are copper with orange and dark brown flecking.

The ventral surface of the head is white with the exception of a scattering of gray melanophores around the edge (Fig. 8C). The gular region has a rosy blush that quickly gives way to a faint yellowish color on the body that grows more intense towards the cloaca. The ventral surface of the tail is an intense goldenrod anteriorly but turns to gray from the midpoint to tip. Scattered orange pigmentation occurs near the edges of the ventral surface of the tail. The ventral surface is free of dark melanophores except near its edges and on the limbs. The undersurfaces of the forelimbs and hindlimbs are light gray, though the left hindlimb does have a few spots of yellow pigment.

In preservation, the dorsum is a grayish-tan color and most of the patterning is faded but still present. Ventral surfaces are a cream coloration and no trace of yellow pigment remains. Eye is opaque.

Description.—The following description is based off of 20 measured individuals. Variation in the 17 ratios for the 20 animals examined is listed in Table 2 (for variation in the 13 morphometric characters see Supplemental Table S2). Molecular variation for six loci is listed in Table 5.

Snout rounded in dorsal view and slightly protruding-to-rounded in lateral view. The snout ranges from 22.6–34.0% (29.1 ± 3.1) of the length of the head. The nares are small and cirri are present in males during breeding season. The eyes are protuberant but barely visible when viewed from the ventral side. Eye diameter is 72.2–108.3% (91.8 ± 9.9) the length of the snout. The interocular distance ranges from 40.4–71.0% (50.5 ± 7.2) of the width of the head. Head width ranges from 56.7–66.0% (60.3 ± 2.7) of the head length, which is 18.9–24.4% (21.5 ± 1.8%) of the SVL.

Total length ranges from 28.5–72.1 mm (52.3 ± 12.2), with SVL ranging from 18–29.5 mm (23.8 ± 3.5). Snout–vent length is 38.1–66.1% (46.6 ± 8.3) of total length. The costal groove count is 14. Forelimbs and hindlimbs are 20.7–26.8% (23.6 ± 1.5) and 24.4–33.5 (27.9 ± 2.2) of the SVL, respectively. The forelimb-to-hindlimb ratio ranges from 76.0–98.5% (84.9 ± 6.4). The manus and pes have four digits each.

The tail length ranges between 33.9–61.9% (53.4 ± 8.3) of the total length. The tail width and height range from 5.0–9.4% (7.0 ± 1.2) and 7.8–10.5 (9.1 ± 0.8) of the SVL, respectively. The tail is round in cross-section throughout the length and no tail keel is present.

Unlike other members of this species complex, coloration and patterning appears less variable, though individuals are still capable of metachrosis. Dorsal coloration can be copper, bronze, or orangish-brown (Fig. 8A–B, D–E). The dorsum can range from nearly patternless to boldly marked with a herring bone pattern. Patterning is usually restricted to the dorsum of the body but can occur on dorsum of the tail,

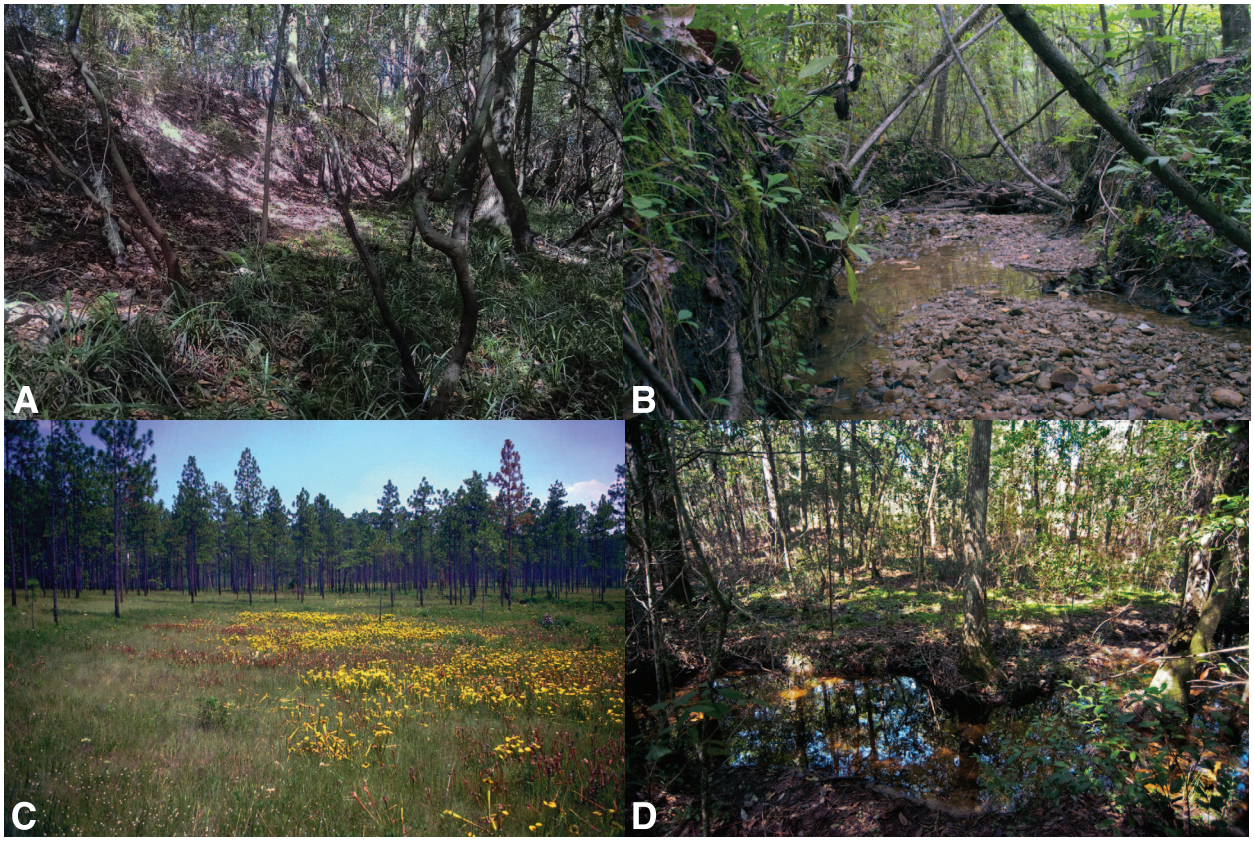

FIG. 9.—*Eurycea quadridigitata* complex. (A) *E. hillisi* type locality: small ravine along Chipola River, Calhoun County, Florida; (B) *E. hillisi* habitat, central Alabama. (C) *E. sphagnicola* type locality: hillside seepage bog, Santa Rosa County, Florida; (D) *E. sphagnicola* paratype locality: hillside seepage bog, Mobile County, Alabama.

though it is often much fainter. The dorsolateral line is chocolate brown, varies from faint to prominent, and has irregular edges. The dorsolateral stripe is commonly most prominent on the posterior half of the body and tail, where it also tends to be widest. Grayish to white flecking is common around the head, below the dorsolateral line, and on the dorsum adjacent to the dorsolateral line.

The ventral surface of the head ranges from gray to white (Fig. 8C, F). This coloration extends onto the body but the extent is variable. Yellow coloration occurs on the underside of the tail and groin area and variably extends anteriorly. Dark melanophores occur variably on the ventral surface but only on the gray or white portions. It is unclear whether the yellow pigment obscures these melanophores or just does not occur in these areas. The peritoneal lining of the gut sometimes shows as a silvery, midventral stripe.

Larva.—We have not examined any larvae that can be attributed to this species and we are unaware of any published works that illustrate or discuss larvae that are attributable to this species.

Etymology.—The specific epithet is a patronym in the genitive singular honoring Dr. David M. Hillis of the University of Texas for his extensive contributions to molecular evolution, phylogenetics, and systematics, his previous work with the genus *Eurycea*, and the many biologists he has mentored that have gone on to make important contributions to our understanding of the evolution of salamanders and phylogenetic systematics in general. We recommend the common name of Hillis's Dwarf Salamanders for this species.

Distribution and natural history.—*Eurycea hillisi* occurs throughout the southern half of Alabama, except the Mobile Bay region and near the Florida border, eastward into mid-central Georgia to the western edge of the Ogeechee River Basin, and between the Chipola and Choctawhatchee rivers of the central Florida Panhandle (Fig. 1). It is known to occur in close proximity with *E. quadridigitata* in the Florida Panhandle and probably does in a broad swath across Georgia and near the Chattahoochee River in Alabama. The westernmost population we are aware of comes to within 60 mi of *E. paludicola* and the hillside seepage species. Further work is needed to determine the full extent of the range of this species including determining (1) how far east it extends in Georgia; (2) whether it ranges into South Carolina; (3) whether it overlaps extensively with *E. quadridigitata* in southern Georgia and the Florida Panhandle; (4) how far west it extends; and (5) how closely it comes in contact with *E. paludicola* and the hillside seepage species.

This species inhabits steephead/ravine systems where it can be found in close proximity to typical *E. quadridigitata* breeding habitat in the floodplains of major creeks and rivers. Gravid females and adult males are often found in first order seepage amongst mats of sphagnum or in leaf packs sitting on top of deep, organic muck along slopes above creek systems (Fig. 9A–B). Given the specific habitats of this animal, we suspect that very little, if any, information

Fig. 10.—*Eurycea quadridigitata* complex. (A) *E. sphagnicola* (UF178811): holotype from Santa Rosa County, Florida; (B) *E. sphagnicola* (UF178811): ventral aspect of holotype from Santa Rosa County, Florida; (C) *E. sphagnicola* (UF178813): paratype from Santa Rosa County, Florida; (D) *E. sphagnicola* (UF178823): adult male paratype from Mobile County, Alabama; (E) *E. sphagnicola*: larva from Santa Rosa County, Florida.

on the natural history and biology of *E. quadridigitata* sensu lato has been based on specimens belonging to this species. A comprehensive study of this species is necessary to determine aspects of its natural history, ecology, and distribution. Collection and detailed description of its larvae are also needed.

Remarks.—See remarks under the account for *Eurycea chamberlaini* concerning the phylogenetic relationships of this species with others in the complex.

Eurycea ***sphagnicola*** sp. nov.
(Figs. 1, 10A–E, 11; Tables 2, 5)

Manculus quadridigitatus quadridigitatus: Mittleman 1947:220. [in part, misidentification]

Manculus quadridigitatus: Mittleman 1967:1. [in part, misidentification]

Holotype.—An adult of unknown sex (UF178811 [DBM 4055], Fig. 10A–B) from "Beautiful Bog," 2.25 mi S of CR 4 and 0.15 mi W of Three Notch Trail, Blackwater River State

Fig. 11.—*Eurycea sphagnicola* (L) and *E. quadridigitata* (R) from ca. 15 mi apart in Santa Rosa County, Florida (Photo courtsey of E. Pierson Hill).

Forest, Santa Rosa County, Florida, 30.840833°N, 86.943333°W, collected 27 September 2016 by D. Bruce Means.

Paratypes.—ALABAMA (n = 10): 10 specimens (UF178819–28 [DBM 4056a–b], Fig. 10D) from unnamed creek, Scoutshire Woods Girl Scout Camp property, Mobile County, 31.04777°N, 88.19222°W.

FLORIDA (n = 7): four specimens (UF178812–5 [DBM 4055, 4058], Fig. 10C) from "Beautiful Bog," 2.25 mi S of CR 4 and 0.15 mi W of Three Notch Trail, Blackwater River State Forest, Santa Rosa County, 30.840833°N, 86.943333°W; three specimens (UF178816–8 [DBM 4057]) from dirt road (D of W20) crossing of Dunn Branch of East Fork Big Coldwater Creek, 0.89 mi W of Three Notch Trail, Blackwater River State Forest, Santa Rosa County, 30.845°N, 86.95444°W.

Referred specimens.—ALABAMA (n = 5): five specimens (UF178892–6 [DBM 3266]) from unnamed creek, Scoutshire Woods Girl Scout Camp property, Mobile County, 31.04777°N, 88.19222°W.

FLORIDA (n = 15): 13 specimens (UF128980–92) from 0.6 mi NW Coldwater Horse Trail Rd and Three Notch Rd., Blackwater River State Forest, Santa Rosa County, 30.84085°N, 86.94941°W; two specimens (UF178973–4 [DBM 3182]) from S of W 20, 0.2 mi W of jct with Three Notch Rd., Blackwater River State Forest, Santa Rosa County, 30.84055°N, 86.94333°W.

Diagnosis.—Small species of *Eurycea* that can be distinguished from all other US plethodontids by the presence of four digits on the pes of hindlimb (five in all other species), except *H. scutatum* and the other four members of this complex. It can be distinguished from *H. scutatum* by the absence of a basal tail constriction and white venter with prominent black spotting. *Eurycea sphagnicola* can be distinguished from the other four species in the complex by the characters listed in the following comparisons section.

Comparisons.—Characters separating *E. chamberlaini* from each of the other members of the species complex are listed herein, followed by character states of other species in parentheses.

Eurycea sphagnicola (n = 36) can be distinguished from *E. chamberlaini* (n = 7) by the following characters (Tables 2, 4, 5): SVL 37.5–51.0% (41.9 ± 3.7) of total length (37.4–63.9% [50.4 ± 11.6]); tail width at base 5.4–10.6% (8.5 ± 1.3) of SVL (4.0–7.2% [5.8 ± 1.0]); tail height at base 8.3–11.9% (10.0 ± 1.0) of SVL (5.0–9.6% [7.6 ± 1.6]); tail round in cross-section (tail laterally compressed); head length 20.0–28.7% (24.0 ± 2.0) of SVL (18.0–21.7% [20.2 ± 1.3]); head depth 7.0–12.4% (9.0 ± 1.3) of SVL (5.6–8.1% [6.9 ± 0.9]); eye diameter 4.9–8.5% (6.3 ± 0.7) of SVL (4.6–5.8% [5.2 ± 0.4]); canthus length 20.7–34.5% (26.4 ± 3.4) of head length (29.8–34.0% [32.3 ± 1.5]); eye diameter 75–127.3% (100.6 ± 13.0) of canthus length (70.6–88.9% [80.6 ± 7.7]); 42 genetic autapomorphies (10 autapomorphies).

Eurycea sphagnicola (n = 36) is distinguishable from *E. quadridigitata* (n = 136) using the following characters (Fig. 11, Tables 2, 4, 5): tail width at base 5.4–10.6% (8.5 ± 1.0) of SVL (4.2–11.2% [7.7 ± 1.3]); tail height at base 8.3–11.9% (10.0 ± 1.0) of SVL (6.3–13.4% [9.2 ± 1.3]); hindlimb length 24.6–35.0% (28.4 ± 2.1) of SVL (21.7–31.9% [26.7 ± 2.3]); forelimb length 19.6–29.1% (24.1 ± 2.3) of SVL (17.0–26.7% [22.3 ± 2.2]); head length 20.0–28.7% (24.0 ± 2.0) of SVL (15.4–24.4% [19.9 ± 1.6]); head width 11.5–15.5% (13.3 ± 1.0) of SVL (8.1–14.2% % [12.0 ± 0.8]); head depth 7.0–12.4% (9.0 ± 1.3) of SVL (5.5–10.5% [7.1 ± 0.8]); interocular distance 5.0–9.8% (6.8 ± 1.1) of SVL (3.9–7.4% [5.5 ± 0.6]); eye diameter 4.9–8.5% (6.3 ± 0.7) of SVL (4.1–6.7% [5.3 ± 0.5]); head width 41.8–64.7% (55.5 ± 3.9) of head length (45.5–77.5% [60.6 ± 5.5]); canthus length 20.7–34.5% (26.4 ± 3.4) of head length (23.2–40.5% [30.7 ± 3.2]); interocular distance 41.4–64.0% (51.4 ± 5.7) of width (32.4–61.9% [46.5 ± 5.2]); ocular diameter 75.0–127.3% (100.6 ± 13.0) of canthus length (64.7–127.3% [88.1 ± 10.0]); 42 genetic autapomorphies (15 autapomorphies).

Eurycea sphagnicola (n = 36) is distinguished from *E. paludicola* (n = 20) by the following characters (Tables 2, 4, 5): 16.4–25.7 mm (22.7 ± 2.2) SVL (22.3–37.2 mm [30.5 ± 4.0]); forelimbs 19.6–29.1% (24.1 ± 2.3) of SVL (18.5–23.8% [21.3 ± 1.5]); hindlimbs 24.6–35.0% (28.4 ± 2.1) of SVL (21.2–31.4% [26.0 ± 3.0]); head length 20.0–28.7% (24.0 ± 2.0) of SVL (17.3–24.7% [19.9 ± 1.8]); eye diameter 4.9–8.5% (6.3 ± 0.7) of SVL (4.3–7.2% [5.7 ± 0.7]); head width 41.8–64.7% (55.5 ± 3.9) of head length (57.9–70.9% [63.3 ± 4.0]); canthus length 20.7–34.5% (26.4 ± 3.4) of head length (27.3–36.1% [32.9 ± 2.6]); eye diameter 75.0–127.3% (100.6 ± 13.0) of canthus length (70.0–100.0% [87.5 ± 10.2]); 42 genetic autapomorphies (48 autapomorphies).

Eurycea sphagnicola is distinguishable from *E. hillisi* using the following traits (Tables 2, 4, 5): tail width at base 5.4–10.6% (8.5 ± 1.3) of SVL (5.0–9.4% [7.0 ± 1.2]); tail height at base 8.3–11.9% (10.0 ± 1.0) of SVL (7.8–10.5% [9.1 ± 0.8]); head length 20.0–28.7% (24.0 ± 2.0) of SVL (18.9–24.4% [21.5 ± 1.8]); eye diameter 4.9–8.5% (6.3 ± 0.7) of SVL (5.1–6.7% [5.7 ± 0.5]); width 41.8–64.7% (55.5 ± 3.9) of head length (56.7–66.0% [60.3 ± 2.7]); 42 genetic autapomorphies (5 autapomorphies).

Description of holotype.—SVL = 24.2 mm; TL = 39.8 mm; TW = 2.3 mm; TH = 2.5 mm; HLL = 6.3 mm; FLL = 4.8 mm; HL = 5.8 mm; HW = 3.3 mm; HD = 2.6 mm; CL = 1.5 mm; IO = 1.7 mm; OD = 1.5 mm.

The head is rounded in dorsal view and slightly protruding in lateral view. The head length is 24.0% of SVL and the width is 13.6% of SVL at the widest point. The head at widest point is 56.9% of the head length and head depth is 10.7% of the SVL. The interocular distance is 51.5% of head at the widest point. The snout is 25.9% of the head length and the eye diameter is 100% of the snout length. The SVL is 37.8% of total length. The tail is complete and is 62.2% of the SVL. The base of the tail is square in cross-section, becoming rounded at distal end. The tail is fractured at a point approximately at the last third of the length. There is no keel evident on the tail. The forelimbs are 19.8% of the SVL with four digits on each manus and the hindlimbs are 26.0% of the SVL with four digits on each pes.

In life (Fig. 10A), the dorsum of the head is a tan color that continues along vertebral region to just posterior of the hindlimb insertion. A coppery-orange coloration appears as smudging on the dorsum of the head, becoming more prominent on the anterior of the body and the dominant coloration at midbody and on the tail. A dark vertebral line is present and faint at the base of the head, becoming more evident toward the tail, but remaining broken. This vertebral line is darkest and most prominent at a point near the

hindlimbs, just above the cloacal region, and then quickly becomes a series of spots on the anterior portion of the tail before disappearing altogether. Some dark smudging exists on the short canthus rostralis, but the dorsolateral stripe only becomes obvious posterior to the eye. The dorsolateral stripe is thin behind the eye, but becomes very thick and darker at midbody and continues so until about the midpoint of the tail, where it becomes faint again until the tip of the tail. There is a grayish coloration under the dorsolateral line from the midpoint of the body to the insertion of the hindlimbs. The dorsal surfaces of the limbs have a tan background overlaid with a series of dark pigmentation. Light gray flecking occurs scattered across the dorsum of the head but is concentrated in the interorbital region, eyelids, and snout. This gray flecking is heaviest below the dorsolateral stripe on the head and body but also occurs on the limbs, lateral surfaces of the anterior part of the tail, and on the upper edge of the dorsolateral stripe.

The ventral surface of the head is white, though scattered dark melanophores occur around the edge (Fig. 10B). The white coloration extends onto the ventral surface of the body to just anterior of the hindlimb insertions, at which point light yellow smudging is present. The yellow coloration replaces the white coloration just anterior to the cloaca and continues onto the first two thirds of the tail. The yellow is replaced by a light gray coloration on the last third of the tail. Scattered grayish melanophores occur on the edges of the ventral surface of the body and tail and occasionally encroach towards the midline. These melanophores are more common on the tail. The underside of all limbs is white with scattered melanophores.

In preservative, the dorsal coloration is faded to a tannish-gray color and most of the dark markings are faint, but evident. The ventral surface is a cream color with no traces of the yellow pigmentation in life. The melanophores are still present but are difficult to discern. The eye is opaque.

Description.—The following description is based off of 36 measured individuals. Variation in the 17 ratios for the 36 animals examined is listed in Table 2 (for variation in the 13 morphometric characters see Supplemental Table S2). Molecular variation for six loci is listed in Table 5.

The snout is rounded in dorsal view and rounded-to-slightly protruding in lateral view. The snout ranges from 20.7–34.5% (26.4 ± 3.4) of head length. The nares are small and cirri are present in males during the breeding season. The eyes are protuberant and only slightly visible when viewed ventrally. Eye diameter ranges between 75.0–127.3% (100.6 ± 13.0) of the snout length. The interocular distance is 41.4–64.0% (51.4 ± 5.7) of head width, which is 41.8–64.7% (55.5 ± 3.9) of the head length. The head length ranges from 20.0–28.7% (24.0 ± 2.0%) of the SVL.

Total length ranges between 38.4–67.1 mm (55.0 ± 6.8) and SVL ranges from 16.4–25.7 mm (22.7 ± 2.2 mm), making SVL 37.7–51.0% (41.9 ± 3.7) of total length. Costal groove count is 12–14. The forelimbs are 19.6–29.1% (24.1 ± 2.3) of the SVL and hindlimbs are 24.6–35.0% (28.4 ± 2.1) of SVL. The forelimb-to-hindlimb ratio ranges from 74.2–97.9% (84.7 ± 5.1). The manus and pes each have four digits.

The tail length is 49.0–62.3% (58.1 ± 3.7) of total length. The tail width and height range from 5.4–10.6% (8.5 ± 1.3) and 8.3–11.9% (10.0 ± 1.0) of the SVL, respectively. The tail at the base is square-like in cross-section, round toward the distal end, and no tail keel is present.

Color and patterning is highly variable in this species, even within a single locality, and animals are capable of metachrosis. Dorsal coloration can be bronze, copper, brownish-orange, or gold (Figs. 10A, C–D, 11). The dorsum may be nearly patternless, with a partial or full vertebral stripe, or with a faint or prominent herring bone pattern consisting of black or dark gray pigment. The dorsolateral stripe is usually black to dark gray. The stripe is usually thinnest and faintest from behind the eye to the forelimbs, at which point it becomes broad and often covers the entire side of the body and tail, though it may fade toward the end of the tail. On some specimens the lateral line becomes a series of thick, vertical bars extending from posterior to the hindlimbs to the anterior portions of the tail. White, gray, or bluish flecking is variably present on the dorsal and lateral aspects of the head, sides of the body, and sides of the tail. These flecks may be present on the dorsum of the body and tail but are usually restricted to the edges of the dorsolateral line.

The ventral coloration of the head is white (Fig. 10B). The white coloration variably extends onto the body where it is ultimately replaced by yellow. The yellow of the venter is usually present at the midpoint but always near the insertion of the hindlimbs and on the tail. The ventral surface of the tail may be entirely yellow or replaced by a grayish coloration near the terminal third. Grayish melanophores are present near the edges of the body and tail, though they may infiltrate towards the midline, especially on the lower half of the tail.

Larva.—The head of larval *E. sphagnicola* are rounded in dorsal profile and protruding in lateral profile (Fig. 10E). The dorsum of the body and head is dark brown with sparse yellow flecking. The lower sides of the head and body are yellowish with a heavy suffusion of dark melanophores. The forelimbs and hindlimbs are dark brown to nearly black with sparse yellow flecking. The posterior sides of the body and first half of tail have large, irregular yellow spots that fade to small, dense yellow spotting near the end of the tail. The iris of the eye is gold with a horizontal bar of black. The tail fins are mottled with dark pigment and small transparent flecks that turn into large spots near the terminal end of the fins. The ventral fin inserts at approximately the anterior third of the tail. The most unique feature of *E. sphagnicola* larvae is that the dorsal tail fin inserts above the cloaca. The dorsal tail fin of *E. chamberlaini* and *E. quadridigitata* inserts anterior to the hindlimbs. The dorsal fin insertion point in *E. hillisi* and *E. paludicola* is unknown; however, if the insertion point is similar to that of *E. chamberlaini* and *E. quadridigitata*, this character could be used to differentiate *E. sphagnicola* larvae from other members of the species complex.

Etymology.—The specific epithet is derived from *Sphagnum*: the generic name for sphagnum moss; Latin suffix *-cola*: inhabitant, dweller; *sphagnicola*: adjective in the nominative singular formed to mean "inhabitant of sphagnum moss"; in reference to the method of finding it within mats of sphagnum in hillside seepage bog areas. We recommend the common name of Bog Dwarf Salamanders for this species.

Distribution and natural history.—*Eurycea sphagnicola* is known from within 50 mi of the Gulf Coast in

Mississippi, Alabama, and the western Florida Panhandle (Fig. 1). It comes in close proximity to *E. quadridigitata* in the western Florida Panhandle (Fig. 11) and at the western extent of its range in Mississippi. On Eglin Airforce Base in Santa Rosa and Okaloosa counties, these two species have been found at different microhabitats on the same hillside. It probably occurs in close proximity to *E. paludicola* in Mississippi. Future work should focus on the northern, eastern, and western limits of the range of this restricted species.

Similar to *E. hillisi*, we doubt little, if any, information from previous studies has been based on populations of this species. This species breeds in dense mats of *Sphagnum* sp. on hillside seepage bogs that are often dominated by other acidic soil-loving plants (e.g., *Sarracenia* sp., *Pinguicula* sp., *Drosera* sp.; Fig. 9C–D). Adults and larvae have been found in these mats at all times of the year, suggesting that this species may not travel far from the breeding habitat, unlike *E. quadridigitata*. Given this information and the fact that this species appears to be the most-geographically restricted of all the members of the complex, an extensive study of its ecology, natural history, and distribution are necessary to determine its conservation status.

Remarks.—This is the most divergent of the eastern species in the complex, having diverged from the clade containing *E. quadridigitata* + *E. chamberlaini* + *E. hillisi* approximately 27–15 Ma. Its preferred breeding sites are sluggish, yet flowing, seepage water, suggesting that this species may represent an intermediate transition between the lotic breeding preference of other *Eurycea* and the lentic preference of *E. quadridigitata*.

Acknowledgments.—We thank J. Apodaca, R. Birkhead, D. Bartlett, B. Bowers, D. Dittmann (Louisiana State University Museum of Natural Science, Genetic Resources), D. Dye, M. Dye, S. Graham, N. Herrera, T.D. Hibbitts, T.J. Hibbitts (Texas Cooperative Wildlife Collection), P. Hill, J. Himes, M. Hollanders, J. Jensen, K. Krysko (Florida Museum of Natural History), C.F. Means, C.G. Means, R. Means, B. Mansell, P. Moler, F. Morrissiey, M. Nordgren, J. Pfaller, T. Pierson, K. Sash, J. Scott, M. Steffen, D. Stevenson, W. VanDevender, S. Wahlberg, J. Williams, L. Wilson, and J. Willson for assistance in acquiring specimens/tissues in the field or via loan. We thank P. Hill (Fig. 11) and K. Roberts (Fig. 7D) for use of their photographs. This work was partially funded through a Florida State University Robert B. Short Grant in Zoology (KPW), Texas Herpetological Society grant (KPW), East Texas Herpetological Society grant (KPW), and National Science Foundation Grant DEB-0841447 (SJS).

SUPPLEMENTAL MATERIAL

Supplemental material associated with this article can be found online at http://dx.doi.org/10.1655/HERPMONOGRAPHS-D-16-00011.S1

LITERATURE CITED

Baird, S.F. 1849. Revision of the North American tailed-batrachia, with descriptions of new genera and species [Including: Descriptions of four new species of North American salamanders, and one new species of scink, pp. 292–294]. Journal of the Academy of Natural Sciences of Philadephia 2:281–294.

Bonett, R.M., M.A. Steffen, S.M. Lambert, J.J. Wiens, and P.T. Chippindale. 2014. Evolution of paedomorphosis in plethodontid salamanders: Ecological correlates and re-evolution of metamorphosis. Evolution 68:466–482.

Camp, C.D., W.E. Peterman, J.R. Milanovich, T. Lamb, J.C. Maerz, and D.B. Wake. 2009. A new genus and species of lungless salamander (family Plethodontidae) from the Appalachian highlands of the southeastern United States. Journal of Zoology 279:86–94.

Carr, A.F. 1940. A contribution to the herpetology of Florida. University of Florida Biological Science Series 3:1–118.

Chippindale, P.T., A.H. Price, J.J. Wiens, and D.M. Hillis. 2000. Phylogenetic relationships and systematic revision of central Texas hemidactyliine plethodontid salamanders. Herpetological Monographs 14:1–80.

Cope, E.D. 1869. A review of the species of Plethodontidae and Desmognathidae. Proceedings of the Academy of Natural Sciences Philadelphia 21:93–118.

Cope, E.D. 1871. Catalogue of Reptilia and Batrachia obtained by C.J. Maynard in Florida. Pp. 82–85 in Annual Report of the Trustees of the Peabody Academy of Science for Years 1869–1870. Salem Press, USA.

Darriba D., G.L. Taboada, R. Doallo, and D. Posada. 2012. jModelTest 2: More models, new heuristics and parallel computing. Nature Methods 9:772.

de Queiroz, K. 1998. The general lineage concept of species, species criteria, and the process of speciation: A conceptual unification and terminological recommendations. Pp. 57–75 in Endless Forms: Species and Speciation (D.J. Howard and S.H. Berlocher, eds.). Oxford University Press, USA.

de Queiroz, K. 2007. Species concepts and species delimitation. Systematic Biology 56:879–886.

Dinno, A. 2016. dunn.test: Dunn's test of multiple comparisons using rank sums. R package Version 1.3.2. Available at https://CRAN.R-project.org/package=dunn.test. Archived by WebCite at http://www.webcitation.org/6lX3qXmp6 on 25 October 2016.

Drummond, A.J., and A. Rambaut. 2007. BEAST: Bayesian evolutionary analysis by sampling trees. BMC Evolutionary Biology 7:214.

Dunn, E.R. 1923. Mutanda Herpetologica. Proceedings of the New England Zoological Club 8:39–40.

Dunn, E.R. 1926. The Salamanders of the Family Plethodontidae. Smith College 50th Anniversary Publication, USA.

Dunn, O.J. 1961. Multiple comparisons among means. Journal of the American Statistical Association 56:52–64.

Fowler, H.W., and E.R. Dunn. 1917. Notes on salamanders. Proceedings of the Academy of Natural Sciences Philadelphia 69:7–28.

Fox, J. 2005. The R Commander: A basic statistics graphical user interface to R. Journal of Statistical Software 14:1–42.

Garman, S. 1884. The North American reptiles and batrachians. A list of the species occurring north of the Isthmus of Tehuantepec, with references. Bulletin of the Essex Institute 16:3–46.

Graham, S.P., and J.B. Jensen. 2011. *Eurycea chamberlaini* (Chamberlain's Dwarf Salamander). Geographic Distribution. Herpetological Review 42:383.

Graham, S.P., G.G. Sorrell, R.D. Birkhead, S.K. Hoss, and C. Raimond. 2008. *Eurycea chamberlaini* (Chamberlain's Dwarf Salamander). Geographic Distribution. Herpetological Review 39:476.

Gray, J.E. 1849. Catalogue of the Specimens of Amphibia in the Collection of the British Museum. Part II. Batrachia Gradientia, etc. Printed by Order of the Trustees. Spottiswoodes and Shaw, UK.

Guindon, S., and O. Gascuel. 2003. A simple, fast and accurate method to estimate large phylogenies by maximum-likelihood. Systematic Biology 52:696–704.

Harrison, J.R., and S.I. Guttman. 2003. A new species of *Eurycea* (Caudata: Plethodontidae) from North and South Carolina. Southeastern Naturalist 2:159–178.

Heled, J., and A.J. Drummond. 2010. Bayesian inference of species trees from multilocus data. Molecular Biology and Evolution 27:570–580.

Holbrook, J.E. 1842. North American Herpetology: Or, a Description of the Reptiles Inhabiting the United States, vol. 5, 2nd ed. J. Dobson, USA.

Holm, S. 1979. A simple sequentially rejective multiple test procedure. Scandinavian Journal of Statistics 6:65–70.

Huelsenbeck, J.P., and F. Ronquist. 2001. MRBAYES: Bayesian inference of phylogeny. Bioinformatics 17:754–755.

International Commission on Zoological Nomenclature. 2000. International Code of Zoological Nomenclature. Article 75.3.1–75.3.7. Available at http://www.nhm.ac.uk/hosted-sites/iczn/code/index.jsp?nfv=true&article=75. Archived by WebCite at http://www.webcitation.org/6ocXEyShc on 28 February 2017.

Jolicoeur, P. 1963. The multivariate generalization of the allometry equation. Biometrics 19:497–499.

Kearse, M., R. Moir, A. Wilson, . . ., A. Drummond. 2012. Geneious Basic: An integrated and extendable desktop software platform for the organization and analysis of sequence data. Bioinformatics 28:1647–1649.

Kozak, K.H., A. Larson, R.M. Bonett, and L.J. Harmon. 2005. Phylogenetic analysis of ecomorphological divergence, community structure, and

diversification rates in dusky salamanders (Plethodontidae: *Desmognathus*). Evolution 59:2000–2016.

Kozak, K.H., R.A. Blaine, and A. Larson. 2006. Gene lineages and eastern North American palaeodrainage basins: Phylogeography and speciation in salamanders of the *Eurycea bislineata* species complex. Molecular Ecology 15:191–207.

Kozak, K.H., R.W. Mendyk, and J.J. Wiens. 2009. Can parallel diversification occur in sympatry? Repeated patterns of body-size evolution in coexisting clades of North American salamanders. Evolution 63:1769–1784.

Kruskal, W.H., and A. Wallis. 1952. Use of ranks in one-criterion variance analysis. Journal of the American Statistical Association 47:583–621.

Lamb, T., and D.A. Beamer. 2012. Digits lost or gained? Evidence for pedal evolution in the Dwarf Salamander complex (*Eurycea*, Plethodontidae). PLoS ONE 7:e37544. DOI: 10.1371/journal.pone.0037544

Leaché, A.D., and M.K. Fujita. 2010. Bayesian species delimitation in West African forest geckos (*Hemidactylus fasciatus*). Proceedings of the Royal Society B: Biological Sciences 277:3071–3077.

Librado, P., and J. Rozas. 2009. DnaSP v5: A software for comprehensive analysis of DNA polymorphism data. Bioinformatics 25:1451–1452.

Macey, J.R., A. Larson, N.B. Ananjeva, and T.J. Papenfuss. 1997. Evolutionary shifts in three major structural features of the mitochondrial genome among iguanian lizards. Journal of Molecular Evolution 44:660–674.

Means, D.B. 2000. Southeastern U.S. Coastal Plain habitats of the Plethodontidae: The importance of relief, ravines, and seepage. Pp. 287–302 in The Biology of Plethodontid Salamanders (R.C. Bruce, R.J. Jaeger and L.D. Houck, eds.). Plenum Publishing Corporation, USA.

Mittleman, M.B. 1947. American Caudata 1: Geographic variation in *Manculus quadridigitatus*. Herpetologica 3:209–224.

Mittleman, M.B. 1967. *Manculus* and *M. quadridigitatus*. Catalogue of American Amphibians and Reptiles 44:1–2.

Moritz, C., C.J. Schneider, and D.B. Wake. 1992. Evolutionary relationships within the *Ensatina eschscholtzii* complex confirm the ring species interpretation. Systematic Biology 41:273–291.

Mosimann, J.E., and F.C. James. 1979. New statistical methods for allometry with application to Florida Red-Winged Blackbirds. Evolution 33:444–459.

Noonan, B.P., and A.D. Yoder. 2009. Anonymous nuclear markers for Malagasy plated lizards (*Zonosaurus*). Molecular Ecology Resources 9:402–404.

Nylander, J.A.A., J.C. Wilgenbusch, D.L. Warren, and D.L. Swofford. 2008. AWTY (Are We There Yet?): A system for graphical exploration of MCMC convergence in Bayesian phylogenetics. Bioinformatics 24:581–583.

Petranka, J.W. 1998. Salamanders of the United States and Canada. Smithsonian Institution Press, USA.

Posada, D. 2004. Collapse, Verion 1.2: A Tool for Collapsing Sequences to Haplotypes. Available at http://darwin.uvigo.es. Archived by WebCite at http://www.webcitation.org/6lX4VTqJV on 25 October 2016.

R Core Team. 2016. R: A language and environment for statistical computing. R Foundation for Statistical Computing, Austria. Available at https://www.R-project.org/. Archived by WebCite at http://www.webcitation.org/6lX4oDKtF on 25 October 2016.

Rambaut, A., M.A. Suchard, D. Xie, and A. Drummond. 2014. Tracer, Version 1.6. Available at http://beast.bio.ed.ac.uk/Tracer.

Rannala, B., and Z. Yang. 2003. Bayes estimation of species divergence times and ancestral population sizes using DNA sequences from multiple loci. Genetics 164:1645–1656.

Ronquist, F., and J.P. Huelsenbeck. 2003. MRBAYES 3: Bayesian phylogenetic inference under mixed models. Bioinformatics 19:1572–1574.

Sabaj Pérez, M.H. (ed.). 2013. Standard Symbolic Codes for Institutional Resource Collections in Herpetology and Ichthyology: An Online Reference, Version 4.0. American Society of Ichthyologists and Herpetologists, USA. 28 June 2013. Available at http://www.asih.org/resources. Archived by WebCite at http://www.webcitation.org/6lX4eTvuy on 25 October 2016.

Sambrook, J., and D.W. Russell. 2001. Molecular Cloning, 3rd ed. Cold Spring Harbour Laboratory Press, USA.

Schmidt, K.P. 1953. A Check List of North American Amphibins and Reptiles, 6th ed. American Society of Ichthyologists and Herpetologists and University of Chicago Press, USA.

Stamatakis, A. 2006. RAxML-VI-HPC: Maximum likelihood-based phylogenetic analyses with thousands of taxa and mixed models. Bioinformatics 22:2688–2690.

Stejneger, L., and T. Barbour. 1923. A Check List of North American Amphibians and Reptiles, 2nd ed. Harvard University Press, USA.

Stephens, M., and P. Scheet. 2005. Accounting for decay of linkage disequilibrium in haplotype inference and missing data imputation. American Journal of Human Genetics 76:449–462.

Stephens M., N.J. Smith, and P. Donnelly. 2001. A new statistical method for haplotype reconstruction from population data. American Journal of Human Genetics 68:978–989.

Swofford, D.L. 2003. PAUP*: Phylogenetic Analysis Using Parsimony (*and Other Methods), Version 4.0b10. Sinauer Associates, USA.

Thawley, C., and S.P. Graham. 2012. *Eurycea chamberlaini* (Chamberlain's Dwarf Salamander). Geographic Distribution. Herpetological Review 43:296.

Timpe, E.K., S.P. Graham, and R.M. Bonett. 2009. Phylogeography of the Brownback Salamander reveals patterns of local endemism in Southern Appalachian springs. Molecular Phylogenetics and Evolution 52:368–376.

Vieites, D.R., M.-S. Min, and D.B. Wake. 2007. Rapid diversification and dispersal during periods of global warming by plethodontid salamanders. Proceedings of the National Academy of Sciences of the United States of America 104:19903–19907.

Wake, D.B. 1966. Comparative osteology and evolution of the lungless salamanders, family Plethodontidae. Memoir of the Southern California Academy of Sciences 4:1–111.

Weisrock, D.W., J.R. Macey, I.H. Ugurtas, A. Larson, and T.J. Papenfuss. 2001. Molecular phylogenetics and historical biogeography among salamandrids of the "true" salamander clade: Rapid branching of numerous highly divergent lineages in *Mertensiella luschani* associated with the rise of Anatolia. Molecular Phylogenetics and Evolution 18:434–448.

Wiens, J.J., T.N. Engstrom, and P.T. Chippindale. 2006. Rapid diversification, incomplete isolation, and the "speciation clock" in North American salamanders (Genus *Plethodon*): Testing the hybrid swarm hypothesis of rapid radiation. Evolution 60:2585–2603.

Wray, K.P., and S.J. Steppan. 2016. Ecological opportunity, historical biogeography, and diversification in a major lineage of salamanders. Journal of Biogeography. DOI: http://dx.doi.org/10.1111/jbi.12931

Yang, Z., and B. Rannala. 2010. Bayesian species delimitation using multilocus sequence data. Proceedings of the National Academy of Sciences of the United States of America 107: 9264–9269.

Zhang, D.X., and G.M. Hewitt. 1996. Nuclear integrations: Challenges for mitochondrial DNA markers. Trends in Ecology and Evolution 11:247–251.

Accepted on 1 February 2017